united nations
educational, scientific
and cultural
organization

international atomic
energy agency

the
abdus salam
international centre for theoretical physics

SMR.1135 - 2

THIRD WORKSHOP ON
THIN FILMS PHYSICS AND TECHNOLOGY
(8 - 24 MARCH 1999)
including
TOPICAL CONFERENCE ON
MICROSTRUCTURE AND SURFACE MORPHOLOGY
EVOLUTION IN THIN FILMS
(24 - 26 MARCH 1999)

"Wear-resistant and low friction coatings: Synthesis, Characterization and Applications"

Yves PAULEAU
INPG-ENSEEG
B.P. 75
1130 Rue de la Piscine
38402 Cedex Saint Martin d'Heres
FRANCE

WEAR-RESISTANT AND LOW FRICTION COATINGS : Synthesis, Characterization and Applications

Yves Pauleau
National Polytechnic Institute of Grenoble
ENSEEG, B.P. 75, 38402 Saint Martin d'Hères Cedex, France
Tel : (33)-4-76-82-65-25; Fax : (33)-4-76-82-66-30; E-mail : yves.pauleau@enseeg.inpg.fr

TOPICAL OUTLINE

I - Wear-Resistant Coatings

1. Introduction
2. Mechanisms of Wear
3. Wear and Friction Tests
4. Factors Affecting Wear Behavior
5. Hardness and Volume of Wear Particles
6. Hard Materials
7. Properties of Hard Transition Metal Nitrides
8. Protective Coatings Produced by Electron Beam Physical Vapor Deposition (EB-PVD)
    - 8.1. Introduction
    - 8.2. Strengthening of Polycrystalline Materials
    - 8.3. EB-PVD Equipment and Experimental Procedure
    - 8.4. Characterization of TiC and TiC/Ti Multilayer Coatings
    - 8.5. Properties of EB-PVD Coatings
    - 8.6. Conclusions
9. Tungsten and Tungsten-Carbon Coatings Deposited by DC Magnetron Sputtering
    - 9.1 Introduction
    - 9.2. Experimental Procedure
    - 9.3. Characterization of Tungsten-Carbon Coatings
    - 9.4. Characteristics of Metal-Carbon Coatings
    - 9.5. Characteristics of Multilayer Coatings for Erosion Tests
    - 9.6. Erosion Rate of Multilayer Coatings
    - 9.7. Conclusions

II - Low Friction Coatings

1. Introduction
2. General Considerations on Friction Between Surfaces
    - 2.1. Friction Coefficients and Amontons Law
    - 2.2. Nature of the Contact Between Two Solid Surfaces
    - 2.3. Friction Between Unlubricated Surfaces
    - 2.4. Friction Between Lubricated Surfaces
3. Basic Mechanisms of Friction
    - 3.1. Role of Shearing and Plowing
    - 3.2. Adhesion Effect on Contact Area
    - 3.3. Effect of Oxide Films on Mechanisms of Friction
    - 3.4. Lubrication Effect of Thin Solid Films
    - 3.5. General Expression of Friction Coefficients

4. Materials for Solid Lubricant Films
    4.1. General Considerations
    4.2. Lamellar Compounds
    4.3. Carbon-Based Compounds
    4.4. Soft Metals
    4.5. Inorganic Materials
5. Rationale for the Selection of Coating Process and Coating Material
6. Conclusions

SOLID LUBRICANT COATINGS PRODUCED BY PHYSICAL AND CHEMICAL VAPOR DEPOSITION TECHNIQUES

Y. PAULEAU
National Polytechnic Institute of Grenoble
ENSEEG, B.P. 75, 38402 Saint Martin d'Hères Cedex, France.
and
CEA - Nuclear Research Center of Grenoble (CENG) - CEREM/DEM - SGSA/LTS, 17 Rue des Martyrs, 38054 Grenoble Cedex 9, France.

ABSTRACT . Solid lubricant coatings are required for lubrication of moving mechanical assemblies operating in hostile environments where conventional fluid lubricants fail. General considerations on friction between surfaces in unlubricated and lubricated sliding contact are presented with a particular emphasis on Amontons' law, nature of the contact and friction phenomena between two solid surfaces. The basic mechanisms of friction which involve shearing and plowing phenomena, adhesion effect on contact area, lubrication effect of oxide films are discussed. The lubrication mechanisms by thin solid films are described on the basis of macroscopic and microscopic approaches. Materials for solid lubricant films namely lamellar compounds, carbon-based compounds, soft metals and other inorganic materials are reviewed. The major advantages and potential interest of solid lubricant thin films produced by plasma-based deposition techniques are highlighted and illustrated by various examples (molybdenum disulfide, amorphous carbon, silver, calcium fluoride and Ag/CaF_2 multilayer films). Finally, the major factors and relevant properties of materials which can be useful to a designer selecting coating process and coating material for a given lubrication application are analyzed in the last section of this paper.

1. Introduction

Adhesion, friction, wear and lubrication phenomena have an impact on many aspects of everyday experience, in particular those related to handling of moving mechanical assemblies, e.g., hinge door, ball bearing, rub seal. Wear of surfaces in relative motion leads to catastrophic failures and represents one of the most costly problems facing industry today. Normally, the word "wear" is used to designate the loss of materials as loose particles produced by mechanical action between contacting surfaces. However, other damage occurring in specific cases can be assimilated to wear, i.e., dimensional changes or roughening caused by metal transfer in the absence of loose particle formation, cracking of brittle noble metal coatings resulting in exposure of base substrates, mechanically-induced flow of material without measurable transfer or loss termed burnishing as can occur with ductile metals. These phenomena are part of the field of tribology which is the study of interacting surfaces in moving contact.

Y. Pauleau (ed.), Materials and Processes for Surface and Interface Engineering,

Numerous options can be considered for solving tribological problems and improving performance of moving mechanical assemblies; these approaches are included in diverse scientific fields such as mechanical design, contact mechanics, solid-state physics, materials science, fluid dynamics, lubrication, surface chemistry, ... In fact, macroscopic approaches coupled with microscopic (atomic scale) investigations of phenomena involved in moving contacts are required for solving many types of friction, lubrication and wear problems. The achievement of a good understanding of tribological contacts which is a crucial point to solve a given engineering problem has become the subject of interdisciplinary research.

In most cases, the structure material appropriate for a given application does not possess the requisite tribological properties, and moreover, for physical or economical reasons, it is impossible to substitute materials with the suitable tribological properties. As a result, the surface of materials in moving contacts has to be covered with coatings able to reduce wear, reduce friction, prevent mechanical damage, and eventually extend the life time of mechanical components. For instance, in sliding contacts without lubrication, non-ferrous alloys of aluminum, magnesium and titanium currently used for aerospace applications are prone to severe wear, i.e., scuffing and galling phenomena (solid-state welding) occur readily. Surface protection through surface treatments is essential when boundary-lubricated or unlubricated contact between these light-weight materials and a counterface is unavoidable [1]. In a sliding contact between a soft base material of hardness, H_s, and a counterface material of hardness, H_c, the wear rate of the soft material depends on the hardness, H_c. Very rapid wear of the soft base material occurs during unlubricated wear tests when the H_c/H_s ratio is of the order of 1.5 and above while with a H_c/H_s ratio in the range 0.72-1.15, the wear is light [2,3]; a ratio value of 0.4 or less is essential for negligible wear rates of the soft material [4]. Accordingly, with a counterface hardness of 6000 to 8000 MPa (Vickers hardness of steel currently used), the wear protection of non-ferrous substrates can be ensured by coatings with a Vickers hardness in the range 15000-20000 MPa, i.e., by hard compounds of refractory metal such as WC, TiC, TiN. With this type of hard coatings applied to a soft base material, the counterface material may experience rapid wear.

Lubrication is well-known to aid in reducing wear of interacting surfaces. In general, sliding friction coefficients much above 0.2 to 0.3 result in irreversible deformation and, hence unacceptable surface damage [5,6]. For conventional applications at or around room temperature, oils and greases are currently employed to reduce friction in moving mechanical assemblies. In hostile environments (vacuum, cryogenic or high temperatures, ionizing radiation, oxidizing or corrosive atmosphere), liquid lubricants fail because of volatility, thermal instability, oxidation or decomposition. Solid lubricant coatings are used in applications for which liquid lubricants are either ineffective or undesirable. Solid coatings which reduce friction might reduce wear rate and enhance durability of mechanical components. Actually, a coating designed for wear and friction reduction in moving contacts is a dual structure composed of a hard material layer for wear protection associated with a (solid or fluid) lubricant layer able to reduce friction. In other words, the solid lubricant coating acts in reducing friction and contributes to prevent damage between contacting surfaces in relative motion. For a successful tribological coating, an additional requirement must be met, i.e., the transfer of both normal and tangential forces involved in the contact should occur through the coating to the substrate without dimensional changes or separation of the coating from

the substrate. Hence, a strong adherence of the tribological coating to the substrate is of prime importance.

From a practical viewpoint, thick coatings are not necessary since a well-designed tribological coating "will not wear". Thin film deposition techniques such as physical vapor deposition (PVD) and chemical vapor deposition (CVD) techniques widely used in various advanced technologies appear as attractive experimental approaches to produce tribological coatings. Highly polished components with optimized precision tolerances can be covered with PVD or CVD thin films as final finish surface treatments. Ion and plasma-assisted deposition processes can be appropriate to obtain the required coating-to-substrate bond strength and correct adherence.

Different classes of materials, deposition processes and properties of hard material coatings susceptible to be included as base layers in tribological coatings were thoroughly reviewed by Sundgren [7]. Now, the purposes of the present chapter are : (i) to discuss various general aspects and basic mechanisms of friction (or lubrication) involved in dry sliding contacts, (ii) to describe the classes of materials used as solid lubricant coatings which can be coupled with hard coatings or deposited on hard substrates, and (iii) to present a rationale for the selection of coating material and coating process for a given lubrication application.

2. General Considerations on Friction Between Surfaces in Unlubricated and Lubricated Sliding Contact

Although friction between objects is a matter of everyday experience, an universal agreement regarding what exactly causes friction does not exist. When a solid slides over another, a number of mechanisms act together in variable proportions depending on experimental conditions used. In fact, the word "friction" is used to account for the gradual loss of kinetic energy occurring in various situations when two solids in contact move relative to one another with a sliding or rolling movement. Low friction is desired for bearings, gears, gimbals; however, in some cases, high friction is necessary, e.g., brakes, clutches, screw threads. Constant, reproducible and predictable friction behavior of materials is required for correct design of mechanical components as well as for efficiency and reliability of moving mechanical assemblies in operation.

2.1. FRICTION COEFFICIENTS AND AMONTONS' LAW

If two solids are in contact with a common plane surface, a friction force tangent to the interface between the solids must be overcome so that one of solids can slide over the other one. In general, a greater force is required for moving one solid initially at rest than for sustaining the motion of one solid relative to the other one. A solid on a flat surface begins to move due to gravity when the surface is progressively raised up to the friction angle, θ. The static coefficient of friction, μ_s, between the solid and the surface is defined as $\mu_s = \tan \theta$. Furthermore, the dynamic or kinetic coefficient of friction, μ, between two solids is expressed by the following ratio :

$$\mu = \frac{F_1}{L_1} = \frac{F_2}{L_2} \qquad (1)$$

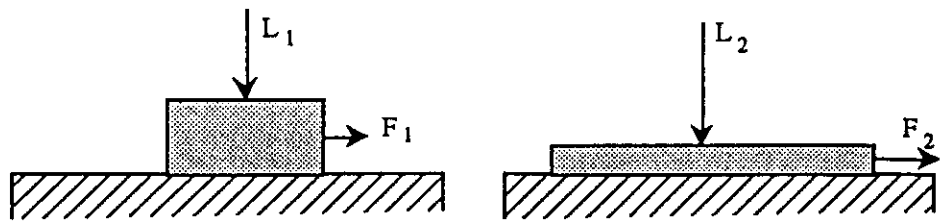

Figure 1. Amontons' law.

where F_1 and F_2 are the friction forces, i.e., the forces tangent to the sliding interface to be applied for moving one solid over another; L_1 or L_2 are the loads or the forces normal to the contact surface (Fig.1). This law, known as Amontons' law, states that the friction coefficient, μ, is independent of the apparent area of contact, i.e., with the same load, L, the friction force, F, is the same for a small sliding block as for a large one. In other words, the sliding friction coefficient, μ, is independent of the load. This law which seems quite contrary to intuitive thinking, was received with some skepticism when Amontons, a French army engineer, presented his findings to the Royal Academy of Sciences in 1699; however, this law is of fairly good general validity.

The tangential (friction) force, F, needed to overcome friction between two solids must be applied over the entire sliding distance. The resulting friction work is equal to the product of the friction force by the sliding distance; this friction energy is dissipated in the form of frictional heating. Thus, friction appears clearly as a process of energy dissipation and must be reduced to improve the energetic yield of mechanical systems and preserve energy.

2.2. NATURE OF THE CONTACT BETWEEN TWO SOLID SURFACES

The friction coefficient in dry sliding contact is essentially determined by properties of materials that reside at the interface. In fact, the friction force depends on the properties of the contacting materials, and the area of contact. During sliding contact, interfacial films often form and control friction phenomena. The friction properties of these interfacial films may be significantly different with respect to those expected from the bulk solids originally placed at the interface.

The surfaces of crystalline materials (even polished metal surfaces) are not really smooth and may have irregular steps of hundreds or thousands of Å in depth. The geometric shape of surfaces is determined by the finishing process or machine used [8]. One can distinguish among macrodeviations, waviness, roughness and microroughness relative to an ideal flat surface (Fig.2). Macrodeviations are caused by lack of accuracy or stiffness of the machining system. Waviness corresponds to sinusoidal undulations (wavelength of 1 to 10 mm and wave height from a few to several hundred μm) caused by low-level oscillations of the machine-tool-workpiece system during machining. Roughness is associated with deviations from the wavy surface caused by geometry and wear of the cutting tool as well as machining conditions and vibrations in the system. Finally, microroughness is a finer roughness superimposed on the surface roughness resulting from internal imperfections in the material or from various surface events such

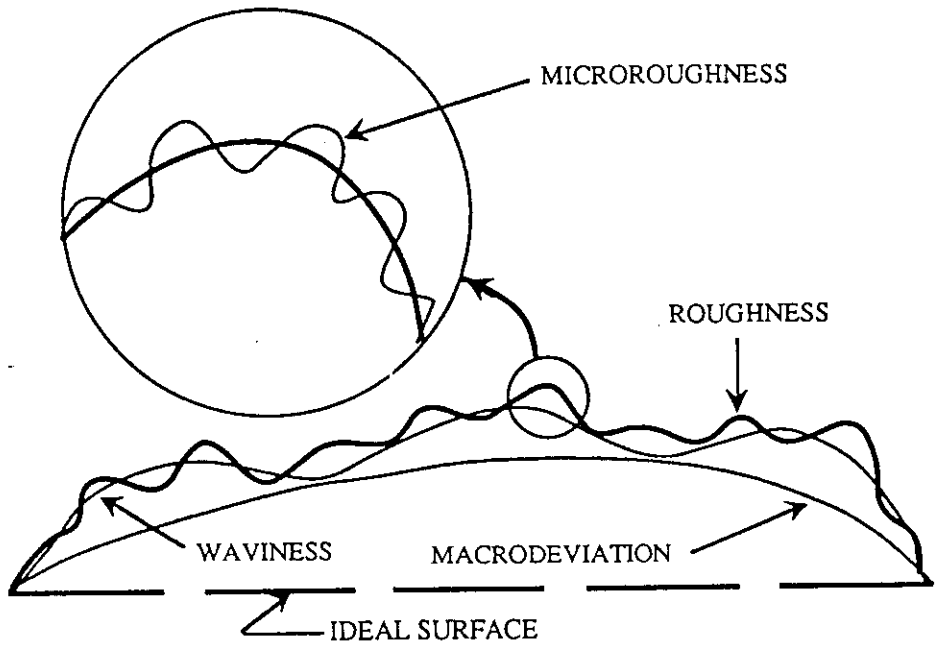

Figure 2 . Various types of surface deviations with respect to the ideal surface.

as segregation, reconstruction, chemisorption and compound formation (Fig.3). In fact, the properties of real surfaces in terms of topography, structure, composition and chemical reactivity are, in general, completely different from those of the ideal surface expected from properties of bulk materials [9].

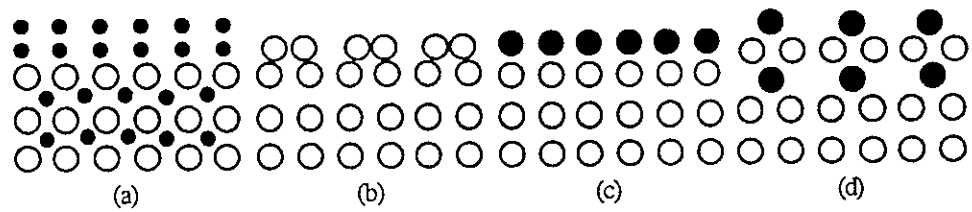

Figure 3. Surface defects created by various processes : (a) segregation, (b) reconstruction, (c) chemisorption, (d) compound formation.

These surface irregularities are expressed in terms of surface roughness determined by profilometer measurements. The average roughness, R_a, is defined as the mean vertical deviation from the centerline whereas the root mean square roughness, R_{rms}, is calculated as the square root of the mean of the squares of the deviations; the root mean square roughness represents the standard deviation of the distribution of the asperity heights. Typical values for R_a and R_{rms} are : 1.4 μm for a fined turned surface, 1.0 μm for a ground surface and 0.2 μm for a polished surface [10].

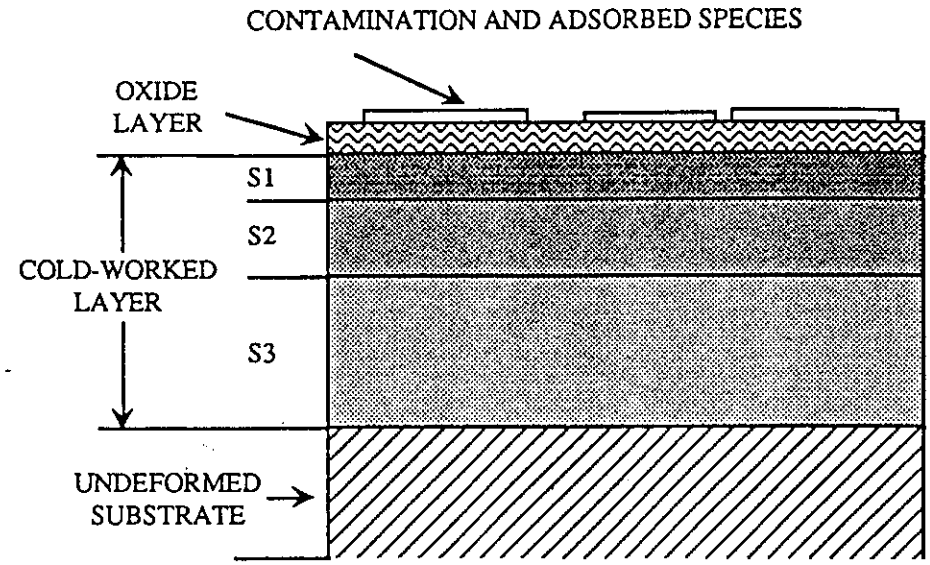

Figure 4 . Schematic representation of the topography and microstructure of a metal surface subject to friction and wear; the cold-worked layer is composed of three zones : (S1) 1-2 μm thick with severe deformation, (S2) 5-10 μm thick with large deformation, and (S3) 20-50 μm thick with minor deformation.

In the case of metals, the surface can be covered with an oxide layer. In addition, for machined and ground surfaces, the microstructure of the subsurface layer is different from that of the bulk metal (Fig.4). During wear, the surface regions of metals experience deformation typically to a depth of about 40 μm; the cold-worked layer may contain segregation, reconstruction and recrystallized zones [11]. Moreover, the outermost zone can be covered with a contaminant layer.

Accordingly, even smooth-appearing surfaces are irregular or deformed on an atomic scale of distances, contain segregations and may be covered with an oxide layer. The nature of surface irregularities can be investigated by atomic force microscopy (AFM) developed by Binnig et al. [12] in 1986. The AFM can be used to image the surface in the weak repulsive or in the attractive modes so that minimum perturbation is introduced by the imaging process itself (Fig.5). This technique provides unique opportunities for model studies of asperity-surface interaction in adhesion, friction, lubrication and wear phenomena [13].

2.3. FRICTION BETWEEN UNLUBRICATED SURFACES

Since real surfaces are not smooth on the atomic scale, the real area of contact between two solids is much smaller than the apparent area of the contacting bodies. In practice, two surfaces brought into contact touch only in isolated regions (Fig.6); the true area of contact can be estimated from measurements of the electrical conductivity between the two solids. For steel surfaces, in a laboratory situation, under a load of 10 kg, the true area of contact, A, is about 0.01 % of the apparent area. Since the real area of contact is much smaller than the apparent area, very high local temperatures can prevail during a

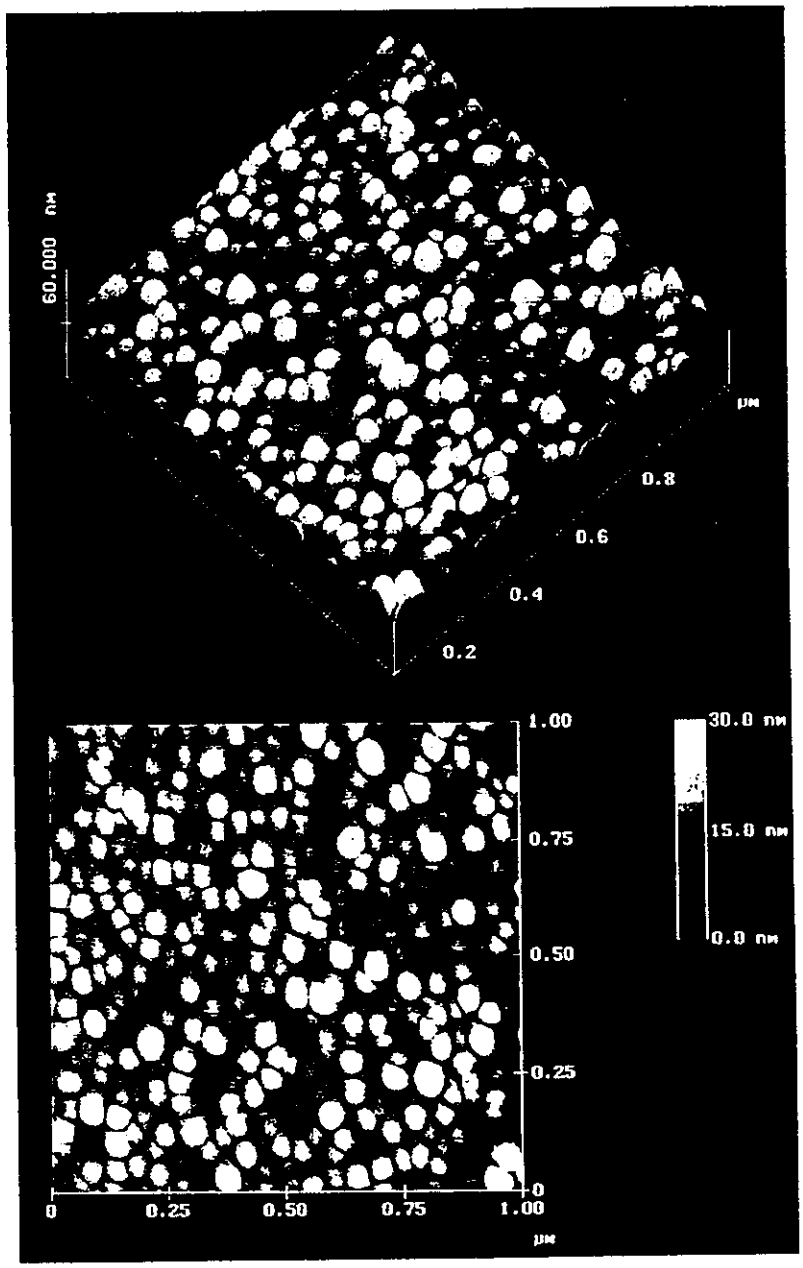

Figure 5. AFM micrographs of 500-nm-thick gold films deposited on glass substrates by thermal evaporation (Courtesy of L. Boyer, Laboratory of Electrical Engineering, Ecole Supérieure d'Electricité, Paris).

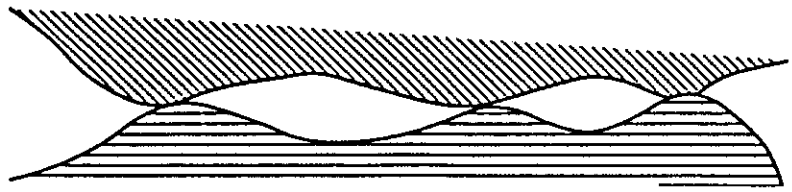

Figure 6. Schematic representation of the real contact surface between two solids.

sliding motion. The temperature rise can be evaluated from the potential difference developed between a rider of one metal sliding against the surface of another one. For a steel rider, the increase in local temperature depends on the counterface material and sliding velocity (Fig.7). The maximum temperature approximately corresponds to the melting point of the lower melting metal. When one of the surfaces is transparent such as glass, the local hot spots can be visualized with an infrared sensitive cell and the local temperature can be estimated from the spectrum of the emitted light; local temperatures as high as 1200°C were reached for steel riders sliding over glass surface [14].

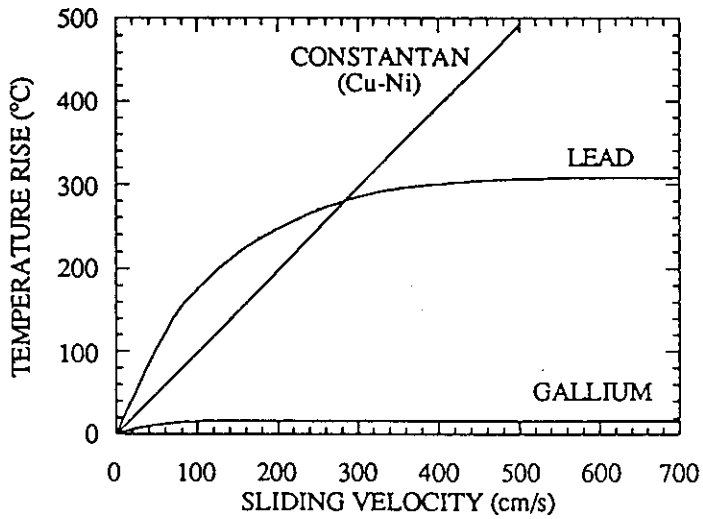

Figure 7. Local temperature rise versus sliding velocity for a steel rider sliding against various metals [22].

Since contact between two surfaces is limited to a small fraction of the apparent area corresponding to surface asperities, local pressures in the contact can reach rather high values. Microscopic examinations of wear tracks left by the rider exhibit portions of the softer metal plucked out by the harder one. Various transformations namely segregation, reconstruction, chemisorption and compound formation can take place at solid surfaces and are promoted by both elevated local temperatures and pressures

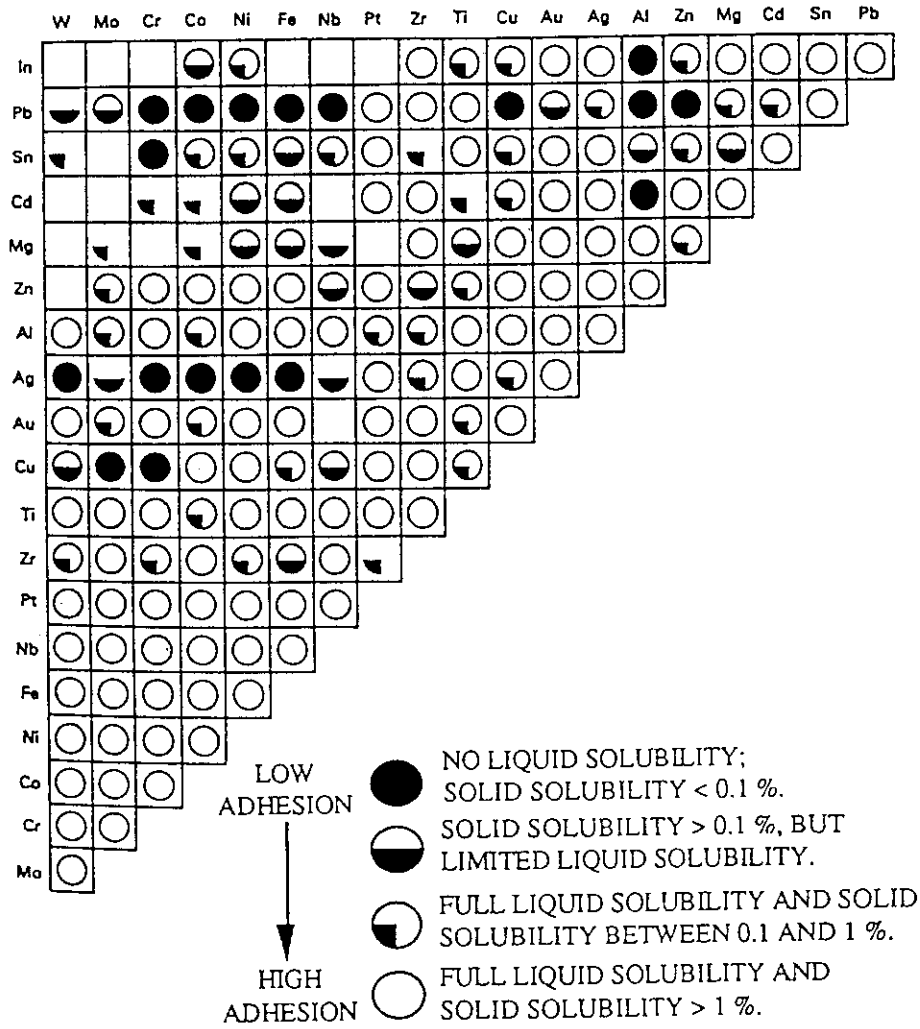

Figure 8. Chart indicating the degree of expected adhesion (and thus friction) between various metal combinaisons based on binary equilibrium diagrams [15].

prevailing in sliding contacts (Fig.3). These transformations may result in significant changes in friction properties which are closely dependent on the surface topography as well as properties of surface and near-surface layers. Segregation phenomena result from the migration of alloy species (in particular light-weight atoms such as carbon) to grain boundaries during processing or heat treatment of materials. The segregation of an alloy element to the surface can dominate adhesion between two surfaces [9]. However, surface segregation can also result in reduced friction, e.g., with certain metallic glasses containing boron, the friction coefficient drops from 1.8-2.5 at 350°C to 0.25 above 500°C as a result of the formation of boron nitride on the surface [9]. Reconstruction

phenomena corresponding to a change in crystal structure may also result in substantial changes in friction coefficient. Interdiffusion promoted by frictional heating may take place and results in compound formation in vicinity of the surface layer. For example, the friction coefficient between one metal sliding against another one that can form solid solution or alloy compounds generally is higher than if the two opposing metals are mutually insoluble. A generalized map showing which metals can safely slide against one another and which metal couples should be avoided was proposed by Rabinowicz [15]; the compatibility chart indicating the degree of expected adhesion (and thus friction between the various metal combinaisons) is reported in Fig.8.

When the surfaces of metallic solids in contact are very clean, interfacial forces can lead to strong adhesion which may dominate friction phenomena. The surface asperities weld together because of atomic bonds form across the interface. This type of adhesion can occur at very low loads. The size of welded area depends on the smoothness of the metal surfaces. With a relatively large real contact area, interactions between surfaces due to interfacial forces strengthen and friction coefficients higher than 5 can be obtained [16,17]. In practice, adhesion between sliding surfaces becomes very strong only for very clean surfaces in high vacuum. The friction coefficient generally drops when molecules that can adsorb on the surfaces such as oxygen or water vapor are introduced in the system. The metal surface is covered with adsorbed species or even with an oxide thin film and the surface area prone for cold welding decreases. This type of behavior can be observed even for non metallic materials such as diamond and graphite; the friction coefficient of 0.5 under vacuum decreases down to 0.2 in air [18].

2.4. FRICTION BETWEEN LUBRICATED SURFACES

To lower friction and protect sliding surfaces against wear, the more straightforward way is to admit a conventional lubricant (oil or grease) in the system. Two distinct regimes can prevail when lubrication is used. In the first case, with a fully hydrodynamic lubrication, the oil film is sufficiently thick to keep the surfaces completely apart; in other words, the contacting materials are essentially independent of each other. Then, the friction is due to viscous dissipation within the lubricant itself, i.e., the friction coefficient depends on the hydrodynamic properties (essentially on the viscosity of the oil) and has little or nothing to do with the specific nature of the solid surfaces. In this situation, Amontons' law is not involved.

As the two surfaces are brought close together by increasing load and reducing relative sliding velocity, the surface asperities begin to come in contact and the lubricant film between the two surfaces becomes thinner. The friction coefficient increases from the very low values possible for fluid lubrication to some value that usually is less than that for unlubricated surfaces. In this regime of lubrication known as boundary lubrication, the nature of the surface region is important.

The degree of separation between two surfaces can be expressed by the ratio, Λ, of the mean gap distance, h, to the composite roughness of the two opposing surfaces, σ :

$$\Lambda = \frac{h}{\sigma} = \frac{h}{\sqrt{\sigma_1 + \sigma_2}} \qquad (2)$$

where σ_1 and σ_2 are the root mean square roughnesses of contacting surfaces. For surfaces with a Gaussian distribution of asperity heights, the value of Λ depends on the

lubrication regime (or inversely). The hydrodynamic lubrication regime prevails if Λ is greater than 3; in this case, asperity interactions in the contact are rather scarce. When Λ is less than 3, asperity rubbing takes place and friction increases as h/σ decreases. Below 1.5, surface deformation may occur and boundary lubrication conditions dominate [19]; in addition, as the mean gap distance, h, diminishes, friction phenomena depend on the behavior of the lubricant thin film interposed between the surfaces and asperity contacts. In the ideal situation, the surfaces would be separated by a lubricant film at all times. As demonstrated by Hardy [20,21], the boundary lubrication could be interpreted in terms of adsorbed films of lubricant; the small friction coefficient values observed in this lubrication regime are caused essentially by the reduction in the force fields between the contacting surfaces as a result of adsorbed films. The ideal lubricant film would exhibit low shear strength between molecular layers parallel to the surface to provide low friction and at the same time, the film must be strongly adherent to the surfaces to prevent intimate contact between opposing solids.

3. Basic Mechanisms of Friction

In the mid-20th century, friction phenomena between solids in relative sliding motion were investigated by Bowden and Tabor and the model proposed by these physicists can be considered as a good starting point for understanding of tribological contacts [5,22]. Their research work focused on adhesion as a major cause of friction. In fact, the concept of cohesive force now called adhesion was introduced by Desaguliers in a presentation to the Royal Society in 1724 and similar ideas were developed by Tomlinson in 1929 and by Hardy in 1936 [23]. According to the Bowden-Tabor model, both adhesion between interacting surfaces and deformation of the subsurface material contribute to the energy dissipation in friction phenomena. In other words, more than the outermost layer of materials which plays a dominant role in adhesion is involved in friction mechanisms.

3.1. ROLE OF SHEARING AND PLOWING

As two solid surfaces are brought together under a given normal load, the real contact area is initially limited to surface asperities and the initial pressure may be extremely large at the few points of contact (Fig.6). In the Bowden-Tabor model, the contacting surface asperities are assumed to deform immediately and this plastic deformation

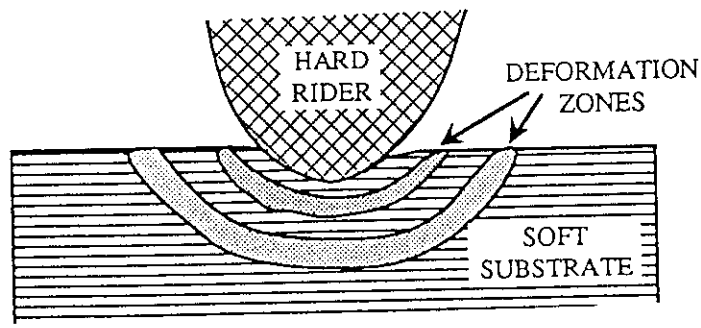

Figure 9. Plastic deformation around a region of contact between two solids.

develops more and more. The total area of contact increases progressively as the time passes and the plastic flow continues until that the local contact pressure has fallen to a characteristic yield pressure, P, of the softer material. In fact, each contact zone exhibits a plastic deformation zone surrounded by an elastic deformation zone (Fig.9).

Hence, according to the Bowden-Tabor model, the real contact area, A, between two solids under a given normal load, L, is determined by the following ratio :

$$A = \frac{L}{P} \tag{3}$$

The values of the yield pressure for metals are in the range 10-100 kg mm^{-2}; thus, with a normal load of 10 kg, the real contact area would be about 10^{-3} cm^2. This value is in good agreement with those deduced from electrical resistivity measurements. However, absolute contact area values can be deduced from Eq.(3) with considerable uncertainties, in particular when work hardening phenomena occur at the contact points. In this case, the yield pressure increases as the deformation continues and the actual yield pressure may be higher than that for the original metal. Furthermore, under very small loads, the pressure limit for elastic deformation is not exceeded and, in this case, the area of contact, A, is not directly proportional to the normal load, L; with a hemispherical rider in contact with a flat surface, the real contact area is proportional to $L^{2/3}$ [24].

In typical tribological measurements such as pin-on-disk tests, a slider or a pin in a fixed position is pressed against a disk rotating about its vertical axis at a given sliding velocity and the friction force, F, to overcome for sliding motion is measured as a function of the number of cycles. Usually, the hardnesses of the pin and disk materials are different. If the harder material is used as a rider, a wear track is plowed in the softer material (Fig.10). In fact, during a sliding motion, the friction work is composed of two

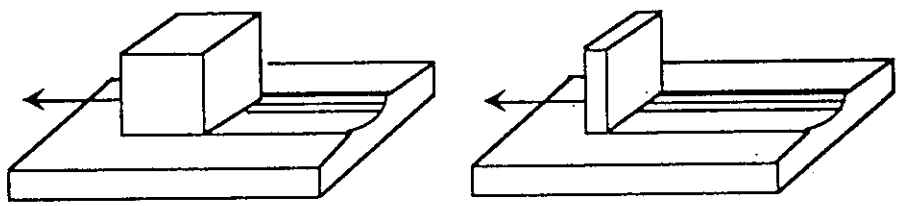

Figure 10. Illustration of : (a) shearing, and (b) plowing actions.

major terms. A first term is necessitated to overcome the adhesion forces and the second work term is associated with the plowing action. As a result, the friction force, F, tangent to the sliding interface and measured during tribological tests, in general, can be split in two terms :

$$F = F_1 + F_2 = A\,s + F_p \tag{4}$$

The force F_1 needed to shear the junctions at the real contact points between the rider and the disk is equal to the product of the real contact area, A, by the shear strength of the interface per unit area, s. The force F_p required for displacement of the softer material

(disk) from the front of the harder one (rider) is expected to be proportional to the cross section area of the plowed track, A'. The plowing contribution is important only when a hard material is sliding against a soft one.

To reduce friction, the shear strength of the sliding interface, the real area of contact and the plowing contribution must be minimized. With a very thin rider as illustrated in Fig.10(b), the contribution of the shearing force, F_1, is minimized, and the contribution of the plowing force, F_2, can be estimated. If the opposing materials are hard, the plowing force, F_p, can be minimized or even neglected. In this case, the tangential force, F, to overcome for sliding motion is equal to the shearing force, $F = F_1 = A\,s$, and the kinetic coefficient of friction, μ, is given by the following expression :

$$\mu = \frac{F}{L} = \frac{A\,s}{L} = \frac{s}{P} \tag{5}$$

Amontons' law is expressed by Eq.(5) in which the terms s and P are the shear strength and the yield pressure of the softer material involved in the sliding contact. According to Eq.(5), the friction coefficient is independent of both the area of contact and the load as established by Amontons in 1699.

The yield pressure and the shear strength for a given metal tend to vary together with the yield stress, σ_y, i.e., P and s are proportional to 3 σ_y and (0.5-0.6) σ_y, respectively. As a result, the universal value of the friction coefficient would be of 0.17 to 0.20. This value is often found for metals in air. However, much higher values are reported for clean metals operating in vacuum, i.e., without protective native oxide layer on the metal surface. In this case, the strength of adhesion forces can be relatively high. In addition, these results suggest that shearing can take place below one of the contacting surface asperities, in particular when one of the materials is weaker than the other, i.e., the weaker material would wear (Fig.11).

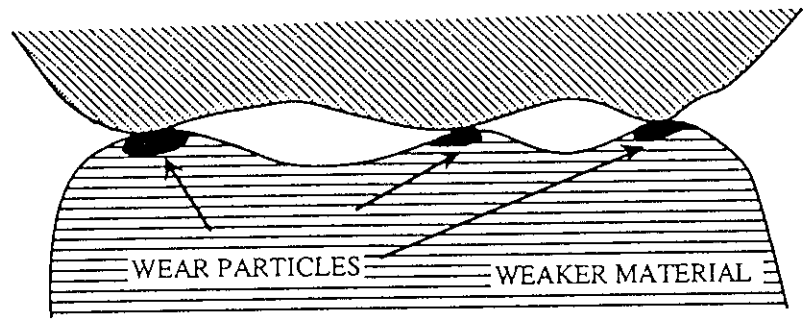

Figure 11. Typical adhesive junctions and wear particle generation in the weaker material caused by friction.

According to this analysis, the friction coefficient for a sliding contact obeys well Amontons' law if neither of the two surfaces is too soft. For instance, the friction coefficient of aluminum on aluminum is constant for load values ranging from 0.037 to 4000 g [22]. Serious complications arise with polymers; the friction coefficient is very dependent on the load since the area of contact is determined more by elastic than plastic deformation. Moreover, the friction coefficient may also depend on the relative velocity

of the two solid surfaces. The local temperature increases with increasing sliding velocity. As a result, the extend of work hardening of metals and the relative importance of the plowing and shearing contributions in the friction force are affected. In general, the friction coefficient tends to decrease with increasing sliding velocity [25,26].

3.2. ADHESION EFFECT ON CONTACT AREA

Adhesion phenomena can occur between two metal surfaces brought into contact under a given normal load. Even if the solids are at rest, microdisplacements of one surface relative to the other resulting in a large increase in contact area are promoted by the load effect. After release of the load, the adhesion is measured by the force required for separation of metals. For instance, after a brief contact between indium surface and a steel ball at rest under a load of 15 g, the force needed to separate the two bodies is about 15 g [27]. The friction coefficient determined by ball-on-disk tribological tests under appropriate conditions was about 5. After sliding tests, the normal force for detachment of the steel ball from the indium surface was equal to 100 g. This large increase in the separation force from 15 to 100 g may arise from the increase in contact area from A_0, contact area for two solids pressed against each other at rest, to A, contact area after sliding tests.

Since the contact area is expected to vary considerably in these experiments, the ratio F/L does not correspond to the kinetic friction coefficient, μ, as defined by Eq.(5). This ratio, F/L, noted Φ, can be related semiempirically to the area change [28]. The contact area, A_0, between two stationary solids pressed against each other is assumed to be given by Eq.(3). Since shear and normal stress are present in the contact, the yield pressure, P, is not directly equal to the pressure resulting from the load; the yield pressure is given by a more general relation :

$$P^2 = P_L^2 + \alpha\, s^2 \tag{7}$$

where α is a constant and P_L is the pressure resulting from the load during sliding tests. The load, L, remains the same in these experiments. As a result, the friction force to cause motion is given by $F = \Phi\, L = A\, s$ where A is the contact area with sliding motion, and the pressure P_L is equal to the L/A ratio so that Eq.(7) can be written as follows :

$$\left(\frac{A}{A_0}\right)^2 = 1 + \alpha\, \Phi^2 \tag{8}$$

Experiments can be designed to estimate the value of α. Namely, a load is applied to two solids at rest in order to establish the contact area, A_0; then, the load is released and the force F_0 required for separation is measured. Under these conditions, the pressure P_L is zero, the force F_0 is given by $F_0 = A_0\, s$, and the contact area A_0 is deduced from Eq.(3), i.e., $L = A_0\, P$ so that the expression of the constant α established on the basis of Eq.(7) can be written as follows :

$$\alpha = \left(\frac{L}{F_0}\right)^2 \tag{9}$$

The value of α depends on the nature of metals in contact. For steel against indium and for platinum on platinum, α was about 3 and 12, respectively [5]. These results do not change the conclusion expressed by Eq.(5), i.e., the kinetic friction coefficient, μ, is given by the ratio of the shear strength to the yield pressure of the softer material involved in the sliding contact. In fact, this analysis tends to demonstrate that with sufficiently strong adhesion between two solid surfaces, the shear occurs in the body of the softer metal rather than at the interface.

Moreover, according to Eq.(8), the contact area A and Φ should increase indefinitely together. For very clean metal surfaces, the contact area enlarges considerably until seizure of surfaces. Usually, the increase in contact area is interrupted by impurities, surface discontinuities and surface structure defects; the contact area becomes a constant and the relative sliding motion of surfaces occurs without particular damage.

To account for adhesion effect in sliding contact, another approach has been proposed by Deryaguin et al. [29]; the friction force is split in two terms :

$$F = \mu L + \mu A P_a \tag{10}$$

The first term is associated with the external load, L. The second term corresponds to an internal force arising from the adhesion pressure, P_a. Many systems exhibiting deviations from Amontons' law would fit Eq.(10) approximately.

3.3. EFFECT OF OXIDE FILMS ON MECHANISMS OF FRICTION

The level of adhesion between two metals depends on the nature of the surfaces and on their affinity for each other or for any adsorbate. Accordingly, depending on the cleanliness of metal surfaces, two opposite situations can be encountered in sliding contacts, i.e., that associated with metal surfaces free of any contamination and that related to metal surfaces covered with adsorbed species or oxide layers.

Very high friction coefficients are measured in vacuum when metal surfaces received previously an in situ cleaning treatment suitable for oxide etching or contaminant elimination; for metals such as tungsten, copper and nickel, the friction coefficient values were found to be in the range 3-6 [30]; a complete seizure of two surfaces of nickel placed in contact and rubbed slightly against each other can occur. This firm metal-metal welding may not happen with two dissimilar metals if these metals are mutually insoluble, e.g., with silver and iron (Fig.8). Furthermore, with very clean metal surfaces, the friction coefficient may be relatively low at the starting point of tribological tests, and very shortly rises to a high value with eventually seizure of metal surfaces. The low value of the initial friction coefficient can be attributed to a lack of ductility which disappears as soon as a local temperature rise is produced by sliding motion.

In air, the behavior of metals in sliding contact is quite different. The friction coefficient between copper surfaces decreases from 6.8 to 0.8 as the exposure time of surfaces to air increases [31]. In addition, the friction coefficient can be dependent on the load. Under very low load values, the oxide film on the metal surfaces is sufficiently

strong for preventing metal-metal contact and the friction coefficient tends to be in the range 0.6-1. Under relatively heavy loads, the oxide film may break down. As a result, metal-metal contacts can occur and increased friction coefficients are observed, e.g., with copper. By contrast, with aluminum, the oxide film is broken even under low loads. Since aluminum is softer than alumina, cracks may appear easily through the oxide film even under low loads. With noble metals such as silver, oxide formation is negligible and the friction coefficient is approximately independent of the load.

In fact, the metal surfaces in air are relatively heterogeneous, i.e., partially covered with an oxide film which may be more or less thin and uniform. According to Bowden and Tabor [32], for such surfaces, the expression of the tangential (friction) force, F, for sliding motion is composed of two terms :

$$F = A\left[\alpha\, s_m + (1 - \alpha)\, s_0\right] \tag{11}$$

In this equation, α is the fraction of metal surface free of oxide or contamination; s_m and s_0 are the shear strengths of the metal and oxide, respectively. With a large surface coverage of the oxide film, α tends to be zero. As a result, under a given load, the friction force and the resulting friction coefficient can be reduced if s_0 is less than s_m. Thus, the oxide film may behave as a solid lubricant film.

3.4. LUBRICATION EFFECT OF THIN SOLID FILMS

A negligible contribution of the plowing force can be obtained from a suitable choice of two antagonistic metals in contact and sliding conditions, i.e., relatively hard metals under moderate loads. In this case, according to Eq.(11), the friction force can be reduced if the surface of one of metals is totally covered with a thin film of solid material having a shear strength lower than the base metal. Under a given load, this reduction in friction force results in reduced friction coefficients; hence, the wear can be minimized and the endurance life of moving mechanical assemblies can be improved. The influence of a solid lubricant film interposed between sliding surfaces can be analyzed either by a macroscopic approach consisting in the determination of the effect of various experimental parameters (lubricant film thickness, load, temperature,...) on the friction coefficient or by a microscopic approach of phenomena taking place at the sliding interface, i.e., deformation of materials and flow of matter.

3.4.1. *Macroscopic Approach of Lubrication Mechanisms by Thin Solid Films*

Various combinations of materials can be distinguished in a sliding contact with a pin-on-disk configuration (Fig.12). Under a given load, with a hard material used as a rider, the friction behavior depends on the relative hardness of the counterface material.

With a soft disk material (Fig.12(1)), the real contact area, A_1, is relatively large while the shear strength of this softer material, s_1, is relatively low. The tangential (friction) force, F, to overcome for sliding motion equal to $(F_1 + F_p) = (A_1\, s_1 + F_p)$ can be relatively high because of the expected plowing contribution, i.e., F_p is not negligible with two opposing materials having very different hardnesses.

With a disk material as hard as the rider (Fig.12(2)), the plowing force is negligible. The friction force, F_2, is given by the product $(A_2\, s_2)$ where A_2 is the real contact area

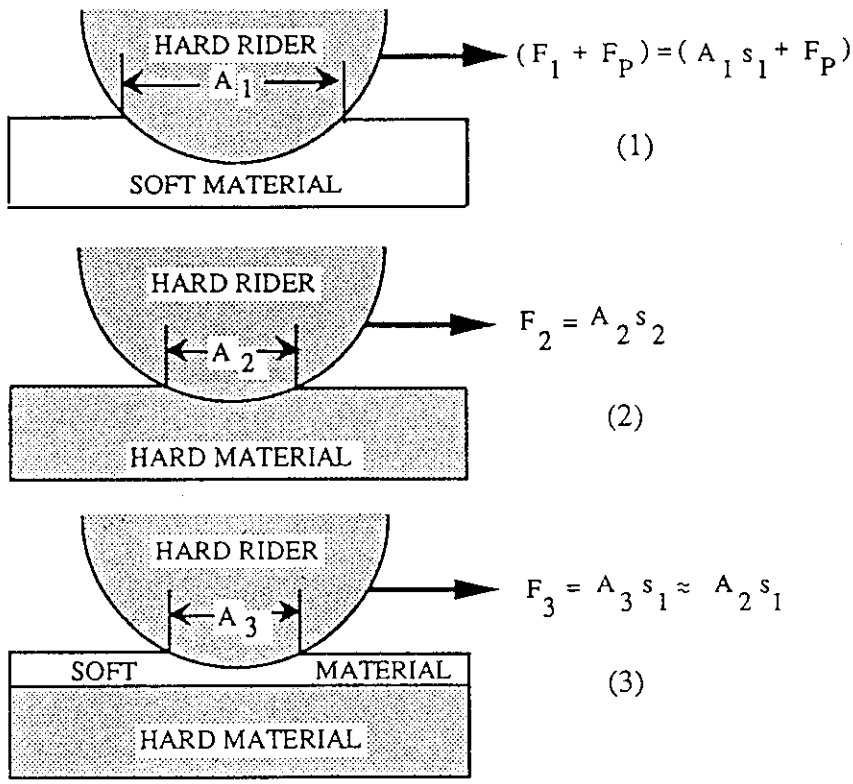

Figure 12. Schematic representation of typical contact situations between two solid surfaces [22].

(lower than A_1), and s_2 is the shear strength of a hard material, i.e., its value is relative high with respect to s_1. Under certain conditions, the friction force, F_2, is lower than F and a reduced friction coefficient can be expected in this situation.

When the hard disk material is coated with a soft thin solid film, the situation can be much more favorable (Fig.12(3)). The plowing action with a thin film firmly adherent to the disk is negligible. In spite of the thin film interposes in the contact, the load is essentially supported by the hard substrate; in other words, a reduced real contact area, A_3, is obtained (its value is approximately equal to A_2). In addition, with a soft thin film, the shearing force depends on the shear strength of the soft material, s_1. As a result, the friction force, F_3, is equal to the product of two terms, A_2 and s_2, with reduced values. Thus, a reduction in friction coefficient can be achieved by interposing a soft thin solid film between two hard materials in sliding contact.

Effect of the Soft Film Thickness. The experimental values of the friction coefficient depend on the soft film thickness as typically illustrated in Fig.13. With smooth surfaces, the minimum friction coefficient is obtained for a critical film thickness of about 1 μm and higher friction coefficient values are provided by thinner and thicker films. With very thin soft films, surface asperities of the substrate can break through

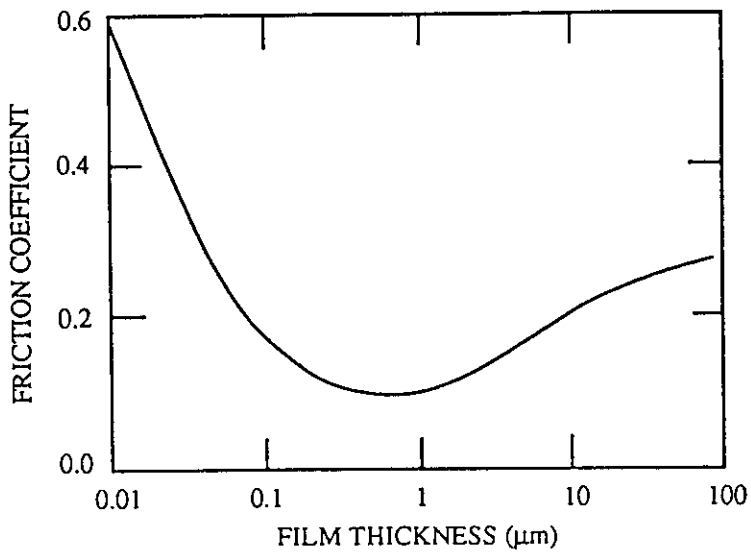

Figure 13. Typical variation of the friction coefficient with the thickness of a soft film deposited on hard substrates sliding against a hard rider.

the film. The increase in friction coefficient with decreasing film thickness below the critical thickness value is attributed to metal-metal contacts established by surface asperities. For thick soft films, a decrease in load-carrying capacity of the surface and a significant plowing action are expected. The friction coefficient is increased by increasing contact area between the slider and the coating and by plowing of the film.

The friction coefficient can be expressed as follows [22,33] :

$$\mu = \beta \frac{s_s}{P_s} + (1 - \beta) \frac{s_f}{P_{f,s}} \qquad (12)$$

where the subcripts s and f refer to the substrate and the film, respectively; the term β corresponds to the fraction of contact area in which interactions between surface asperities occur. In Eq.(12), the first term corresponds to the contribution of the substrate while the second term represents the contribution of the film-substrate combinaison, i.e., the pressure $P_{f,s}$ can vary from P_s (value equal to the yield pressure or hardness of the original substrate) with a thin soft film deposited on the hard substrate to P_f (yield pressure or hardness of the film material) for a thick soft film. A more general theory for the friction mechanism of thin solid films proposed by Halling [34,35] fits well various experimental results. However, the theoretical expression of the friction coefficient contains several parameters not always easy to determine experimentally.

Load Effect. According to Amontons' law, the friction coefficient is independent of the load; this law holds for many combinaisons of materials [22]. However, for certain solid

lubricant films such as polymer films [36,37] and inorganic films [38] on hard substrates, a load dependence of the friction coefficient is commonly found.

In fact, the shear strength can be dependent on the pressure. At high pressures, the relationship between the shear strength, s, and the pressure, P, can be expressed by [36,37] :

$$s = s_0 + \alpha P \tag{13}$$

As a result, the expression of the friction coefficient can be written as follows :

$$\mu = \frac{s}{P} = \frac{s_0}{P} + \alpha \tag{14}$$

The Hertzian contact pressure, P, is given by the load to the apparent contact area ratio. For an elastic deformation of materials in contact or for a contact between two nonconforming surfaces (i.e., with concentrated contact points), the Hertzian pressure depends on the load, L, i.e., is proportional to L^n with n = 1/3 for a circular contact and n = 1/2 for a cylindrical (line) contact [18]. For Hertzian contacts, the difference (μ - α) is proportional to (s_0 L^{-n}). As illustrated in Fig.14, the Hertzian contact behavior accurately describes the load dependent friction coefficient for MoS_2 [18].

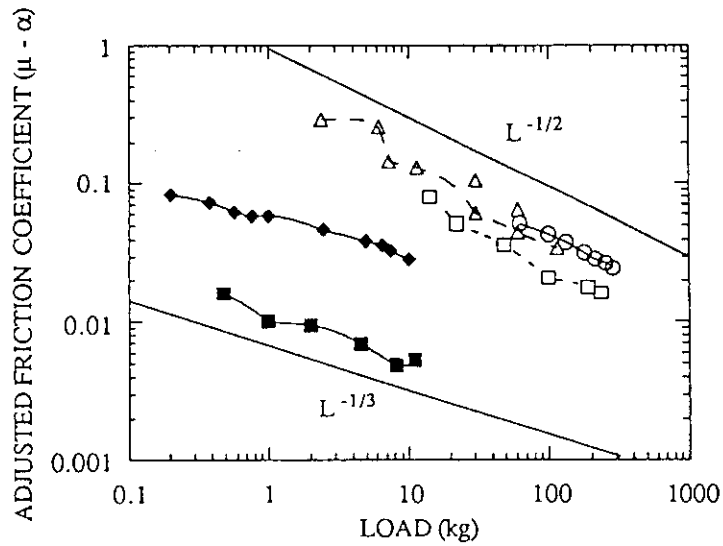

Figure 14. Dependence of the adjusted friction coefficient (μ - α) on the load of MoS_2 with a ball-on-disk geometry (■) (◆), and a cylinder-on-disk geometry (□) (△) (○) [18].

For a smooth ball sliding on a hard flat substrate under loads below the elastic limit, the contact area is determined by the Hertzian equation. In this situation, the friction coefficient can be expressed by the following equation [39] :

$$\mu = \frac{s_0 \pi}{L^{1/3}} \left(\frac{\beta R}{4 E} \right)^{2/3} + \alpha \qquad (15)$$

where R is the radius of the ball and E the equivalent elastic modulus of the opposing materials. Eq.(15) shows that for achieving low friction, the film material must possess a low shear strength and must be deposited on material surface of high hardness or high elastic modulus. This type of contact was achieved with a steel ball sliding on a smooth steel plate covered with a MoS_2 thin layer; a friction coefficient as low as 0.02 was measured [39,40]. Friction measurements performed under Hertzian contact conditions can be used to determine s_0 and α values (Table I). Reliable values of s_0 can be obtained; however, it is not clear whether these numbers correspond to the shear strength of the film or of the interface itself.

Effect of Other Test Conditions. In general, the friction coefficient decreases with increasing test temperature. This variation can be attributed to the increased softening of materials at high temperatures. A direct correlation between the friction coefficient and the bulk strength can be noticed for silver (powder) [41]. However, for some materials, the friction coefficient decreases or increases considerably at certain temperatures [41].

Table I. Shear strength measurements on solid lubricant films; $s = s_0 + \alpha P$ [18].

FILM	s_0 (MPa)	α
Sputter-deposited MoS_2 (in dry air)	25	0.001
Diamond-Like Carbon (in dry air)	25	0.010
B_2O_3 (in 50 % RH air)	23	0.006
Sputter-deposited MoS_2 (in vacuum)	7	0.001

The decrease in friction coefficient with increasing temperature may result from local melting of the lubricant material [42] whereas an increase in friction coefficient generally originates from film failures caused by oxidation or by poor film-substrat adherence.

A decrease in friction coefficient can be observed with increasing sliding velocity. This friction behavior is, in general, attributed to the temperature rise caused by frictional heating in the contact [18].

The nature of gas atmosphere can affect considerably the friction and wear behavior of solid lubricants. For example, MoS_2 and diamond-like carbon films exhibit very low friction coefficients in the range 0.01-0.02 in vacuum while in air much higher values of about 0.20 can be obtained; the reverse situation is encountered for graphite and diamond; the friction coefficient decreases from 0.50 in vacuum to 0.20 in air [18]. This effect of gas atmosphere demonstrates that the surface chemistry can play a key role in friction process.

Furthermore, the endurance of a solid lubricant film can be dependent on the atmosphere; however, there is no general trend of endurance with friction coefficient. For instance, the endurance of MoS_2 thin films decreases as the friction coefficient decreases, i.e., as the load increases. Generally, solid lubricant films can exhibit very

low wear rates and acceptable endurance lifes, e.g., less than a fraction of an atomic layer can be stripped away per pass. In this case, 1-μm-thick solid lubricant films may survive a million or more passes.

3.4.2. *Microscopic Approach of Lubrication Mechanisms by Thin Solid Films*

According to the previous analysis of sliding contact, low friction coefficients can be achieved with hard antagonistic substrates covered with "selected" solid lubricant films operating under "appropriate" sliding conditions. Now, a microscopic approach of various processes taking place at the contact interface is required for a good understanding of friction mechanisms involved in this type of contacts. In other words, the study of deformation and flow of matter in contact, i.e., the study of the interfacial rheology is necessary to understand the lubrication mechanism.

Schematically, the solid lubricant film (or coating) may accomodate to sliding by three possible ways as illustrated in Fig.15 [43]. With a solid film firmly adherent to the disk as well as to the rider, a flow of matter can occur inside the film to accomodate relative displacements of the two bodies (Fig.15(1)). Normally, this type of "intrafilm flow" is associated with noncrystalline materials. However, viscous-like shear flow can also occur with crystalline materials at sufficiently elevated temperatures.

When the solid film is adherent only to the disk, the sliding displacement takes place at the rider-film interface (Fig.15(2)). This type of "interface sliding" has not been demonstrated definitely in pin-on-disk tribological tests. However, this sliding mode may occur under low loads with very smooth sliding surfaces.

Another sliding mode can be active if the solid lubricant film adheres strongly to both the rider and disk (Fig.15(3)). The film can split in two distinct films sliding against one another. In this type of "interfacial sliding" neither of the two original surfaces is in contact, and the friction coefficient is dependent on the shear strength corresponding to a sliding contact between the two films.

These three sliding modes can be active successively in sliding contact. With a solid lubricant film adherent to both rider and disk surfaces, the sliding motion begins with intrafilm flow or interface sliding mode. The film experiences wear, loose particles are pushed out the wear track and the film begins thinner. Then, a steady state is reached in which interfilm sliding may become the dominant sliding mode.

In some cases, the situation can be more complex. During sliding motion, the solid lubricant film undergoes flow and new parts of the films are exposed to the surrounding atmosphere. A "third body" can form at the interface and accomodate relative motion of two solid surfaces [44,45]. The formation of the interfacial film or compound can be predicted and analyzed by a thermodynamic study of the sliding system. The model for interfacial film formation proposed by Singer [46] is illustrated schematically in Fig.16. After a few cycles, a thin layer is removed from the film and transfers to the rider, e.g., the native oxide film on the surface of the lubricant film (Fig.16(1)). The transfer layer can react with surrounding gas as well as with the rider material if the local temperature rises sufficiently (Fig.16(2)). After a larger number of cycles, the transfer layer thickens, and debris particles break and fall onto the wear track (Fig.16(3)). Then, these debris particles can play a dominant role in friction and wear behavior, e.g., abrasive wear may occur in the contact.

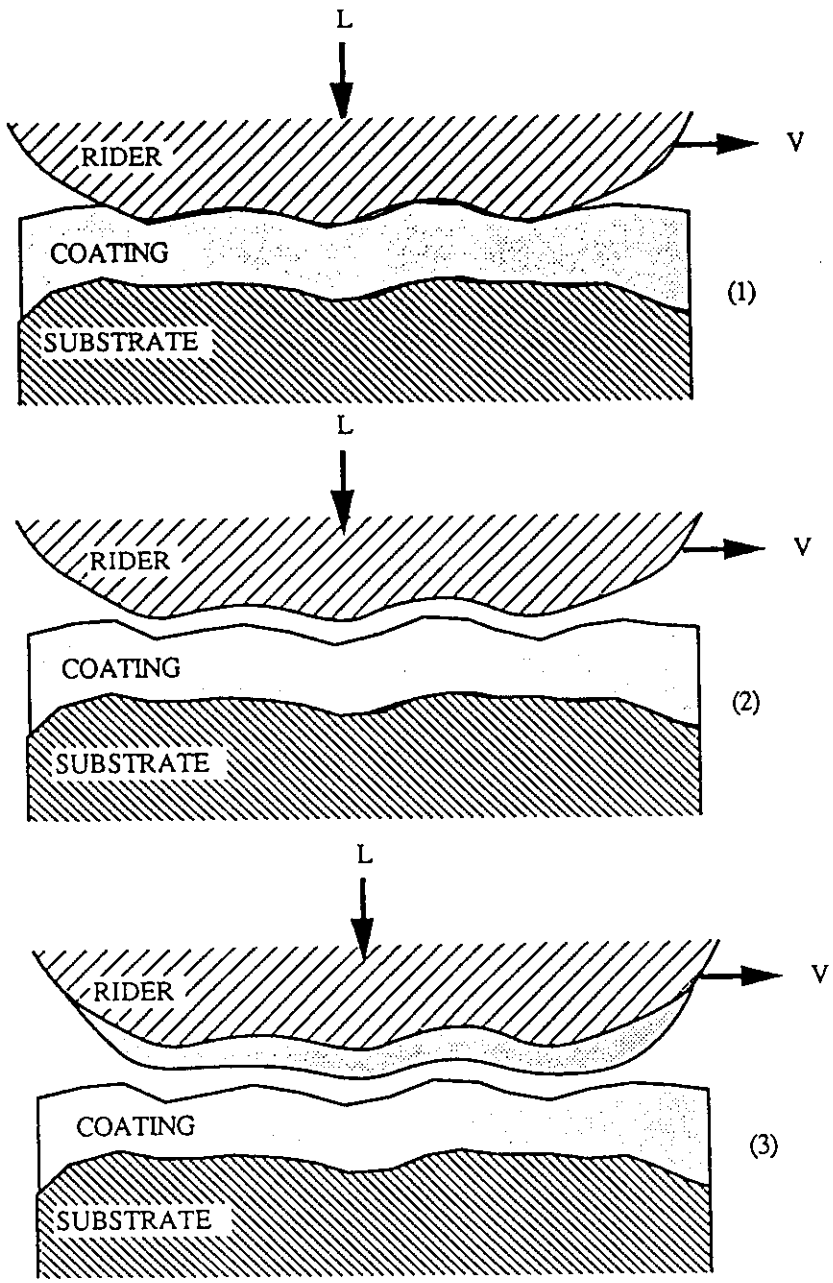

Figure 15. Possible ways of sliding accomodation between a rider and a substrate covered with a solid lubricant coating : (1) intrafilm flow, (2) interface sliding, and (3) interfacial sliding with transferred coating [43].

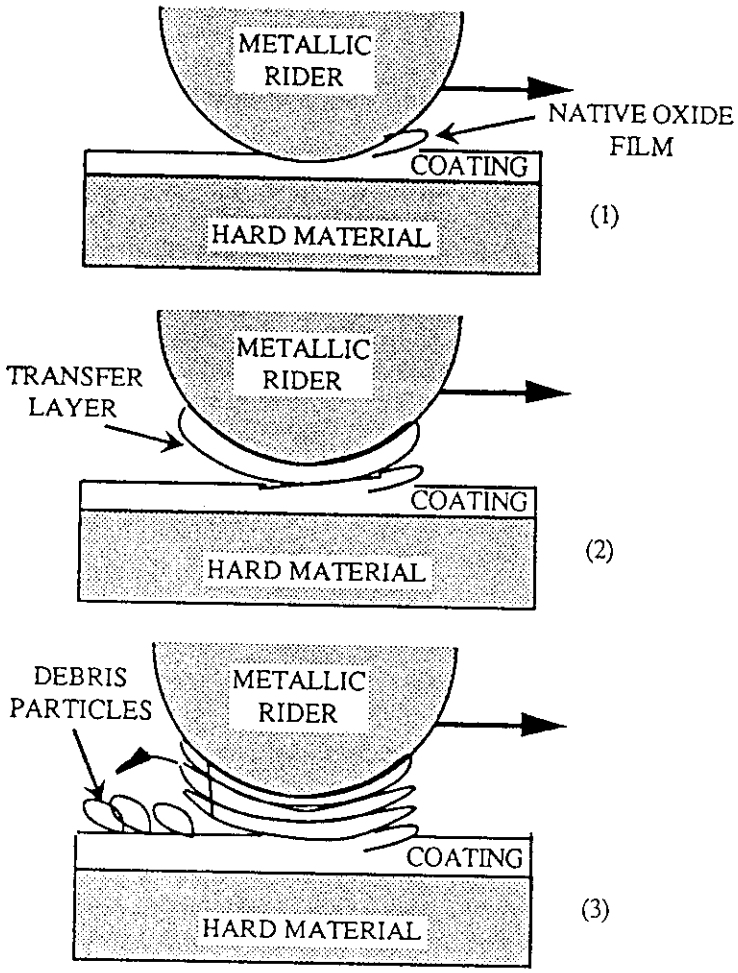

Figure 16. Schematic representation of the formation of the interfacial film (third body) and wear debris in reactive ambient gas (oxygen) [46].

3.5. GENERAL EXPRESSION OF FRICTION COEFFICIENTS

According to various phenomena which can be involved in friction mechanisms, the friction coefficient between two solid surfaces in relative sliding motion can be expressed by a general equation composed of four different terms :

$$\mu = \mu_a + \mu_p + \mu_e + \mu_t \qquad (16)$$

The term, μ_a, is associated with adhesion phenomena (or spot welding) in the contact zone. The contribution of μ_a is relatively high for very clean surfaces sliding

against one another in high vacuum. Under these conditions, for certains metals, the seizure of surfaces can occur and the moving mechanical assembly is totally jammed. Under normal operation conditions, adhesion plays only a minor direct role; however, the adhesion effect can be significant on the plastic deformation occurring for plowing action.

The second term, μ_p, corresponds to the contribution of plastic deformation and plowing action occurring when a metal with hard surface asperities slides against a softer metal. Permanent grooves form in the surface of the softer material or a "bow wave" of soft material is pushed ahead of the hard rider across the surface.

The term, μ_e, accounts for the effect of the elastic deformation of the material below the plastically deformed zones (Fig.9). The contribution of this term is more significant as the surfaces are cold worked and smoothed during the run-in period.

The last term, μ_t, corresponds to the effect of third body particles interposed between the moving surfaces after a certain sliding distance. Small wear particles can agglomerate and indent the surfaces or roll between them. These particles are active in plastic deformation of materials in contact.

The relative contribution of these four terms varies, in general, during sliding operations. In addition, various phenomena occurring in sliding contact can be coupled and these four different terms might not be totally independent.

4. Materials for Solid Lubricant Films

4.1. GENERAL CONSIDERATIONS

The interest of scientists in solid lubricant materials is of relative recent origin. After the initial patent listing lubricants including MoS_2 suitable for various uses in 1939 [47], the earliest substantial results on molybdenite, MoS_2, as a new lubricant in vacuum were reported in 1941 [48]. The demand for advanced vacuum technology and lubrication in extreme environment, in particular for aerospace applications was incentive to research and development programs on solid lubricant materials. A review of the fundamental knowledge on molybdenum disulfide as a lubricant was published in 1967 [49]. More recently, extensive review papers on solid lubrication were authored by Sliney [50,51], Lancaster [52], Sutor [53] and Singer [54].

Various requirements must be met for application of solid materials as solid lubricants in sliding contact. Firstly, to provide low friction coefficient, the solid lubricant must have a low shear strength in the temperature range of the application. As described in the microscopic approach of friction mechanisms, intrafilm flow can occur to accomodate relative displacements of two bodies in contact. With crystalline materials, shear occurs by slip along preferred crystallographic planes and a severe plastic intrafilm flow is observed when the film adheres strongly to the lubricated surfaces. In fact, low shear strength is not sufficient to ensure reliable lubrication; very strong adherence between the lubricant film and the substrate is of paramount importance. Furthermore, a low abrasivity of solid lubricant materials is needed to avoid rapid abrasive wear of lubricated surfaces by loose particles of solid lubricant. This characteristic is a function of the lubricant hardness to the bearing material hardness ratio. This abrasive wear by loose lubricant particles can be minimized with lubricant materials softer than the base substrates. Finally, the solid lubricant material must be

stable in the environment of tribological applications as well as under storage conditions.

Different classes of potential solid lubricants are listed in Table II. This large variety of solid materials can be deposited on substrates by a number of thin film deposition techniques. During pioneering works on solid lubrication, various techniques were investigated to apply powdery lubricant materials on contact surfaces. For instance,

Table II. Potential solid lubricant materials.

Lamellar solids	dichalcogenides (MoS_2, WS_2, $MoSe_2$, ...) graphite, intercalated graphite $[(CF_2)_n]$ BN, $CdCl_2$, $PbCl_2$
Carbon-based compounds	graphite, diamond, diamond-like carbon (DLC) amorphous carbon (a-C:H), polymers (PTFE)
Soft metals	Au, Ag, Pb, Sn, In
Inorganic compounds	fluorides (Ca, Ba, Li, rare earths) oxides (Cd, Cu, Pb, Co) sulfides (Bi, Cd)

MoS_2 layers can be prepared by burnishing or bonding processes. Burnished lubricant layers are prepared by a rubbing process that transfers the powdery lubricant material onto the surface to be coated (Fig.17). The adherence, surface coverage and thickness of burnished layers are difficult to control and reproduce; in addition, these characteristics are strongly dependent upon the preparation of the substrate surface and rubbing procedures. The lubricant transfer can be non uniform so that lubricant bumps and bare regions can appear on the surfaces. In some cases, a brushing process is needed to remove thick or loose material and form acceptable thin layers. In general, these burnished layers exhibit poor adherence to substrates and relatively short endurance life compared to coatings of MoS_2 or other lubricant materials prepared by other methods.

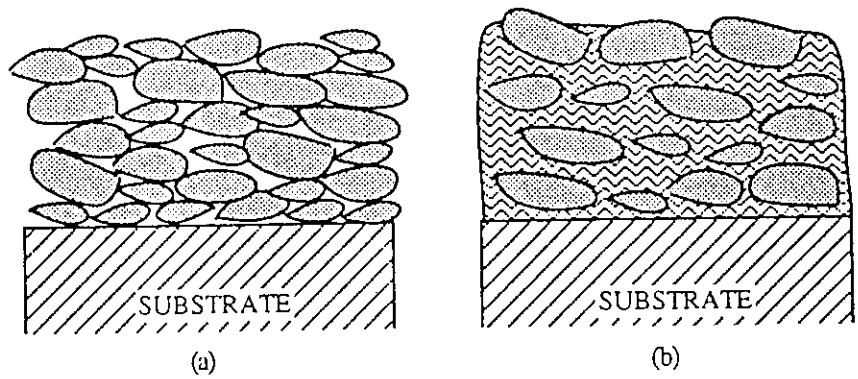

Figure 17. Schematic representation of : (a) a burnished MoS_2 layer, and (b) a bonded MoS_2 layer.

A mixture of powdery solid lubricant such as MoS_2 with an inorganic or organic binder and a solvent can be applied to surfaces to be coated by dipping, painting or spraying. Then, the solvent is removed by either air or heat curing to produce bonded layers (Fig.17). In this technique, appropriate treatments of the original substrate surface (grit blasting, anodization, ...) can be necessary to improve the adherence of layers. The use of a binder results in improved adherence and endurance life of lubricant layers with respect to those of burnished layers. In fact, the bonded layer consists of a binder matrix associated with a solid lubricant. The minimum friction coefficient is obtained by enrichment of the composite surface with lubricant during sliding operations.

Moreover, various techniques including powder metallurgy processes were developed to produce composite bearing materials in which the solid lubricant is dispersed throughout the structure. For example, a composite composed of a porous sintered metal (nickel-chrome alloy) matrix infiltrated with barium fluoride-calcium fluoride eutectic as lubricant materials exhibit low friction coefficients and wear rates at high temperatures [55]. However, these composites are difficult and time consuming to prepare. For high temperature applications, fluoride-based lubricant materials have been applied to surfaces as ceramic-bonded coatings using a porcelain enameling process and fusion-bonded all-fluoride coatings [51]. Composite lubricant coatings with similar compositions can be prepared more conveniently by plasma spraying techniques [50].

In general, bonded layers and other coatings of several μm or hundred μm thick do not exhibit the lowest possible friction coefficient and are too thick for lubrication of polished components with optimized precision tolerances. Physical and chemical vapor deposition techniques presented in detail by Rigsbee [56] and Wahl [57], respectively, are of major interest to prepare thin films of solid lubricant materials required for lubrication of precision components operating in hostile environments. Moreover, PVD and CVD techniques are known to provide materials such as diamond-like carbon films with specific properties which are difficult or even impossible to obtain from films produced by powder metallurgy methods or other deposition techniques.

An exhaustive presentation of methods of preparation and friction properties of lubricant materials listed in Table II would be a very long and cumbersome lecture. In fact, the major advantages of these solid lubricants as well as the potential interest of plasma-based deposition techniques in preparation of thin films of these materials can be highlighted by some examples correctly selected and described in detail in the next sections.

4.2. LAMELLAR COMPOUNDS

Dichalcogenides (disulfides, diselenides and ditellurides) of group IV B, V B and VI B metals (e.g., Mo, W, Nb, Ta) crystallize with a highly anisotropic layer structure. For instance, the structure of MoS_2 is composed of stacked atomic planes (Fig.18). Each layer or lamella consists of two planes of S atoms and one intermediate plane of Mo atoms; in these planes, atoms are arranged in hexagonal arrays. The distance between the planes of Mo and S atoms belonging to a lamella is 1.54 Å. Within a lamella, the atoms are tightly bound by covalent bonds whereas weak van der Waals bonding exists between S planes of two adjacent lamellae. The distance between these two adjacent S planes belonging to two distinct lamellae is about 3.08 Å. In other words, attraction forces between the two adjacent S planes are weak whereas strong covalent bonds exist

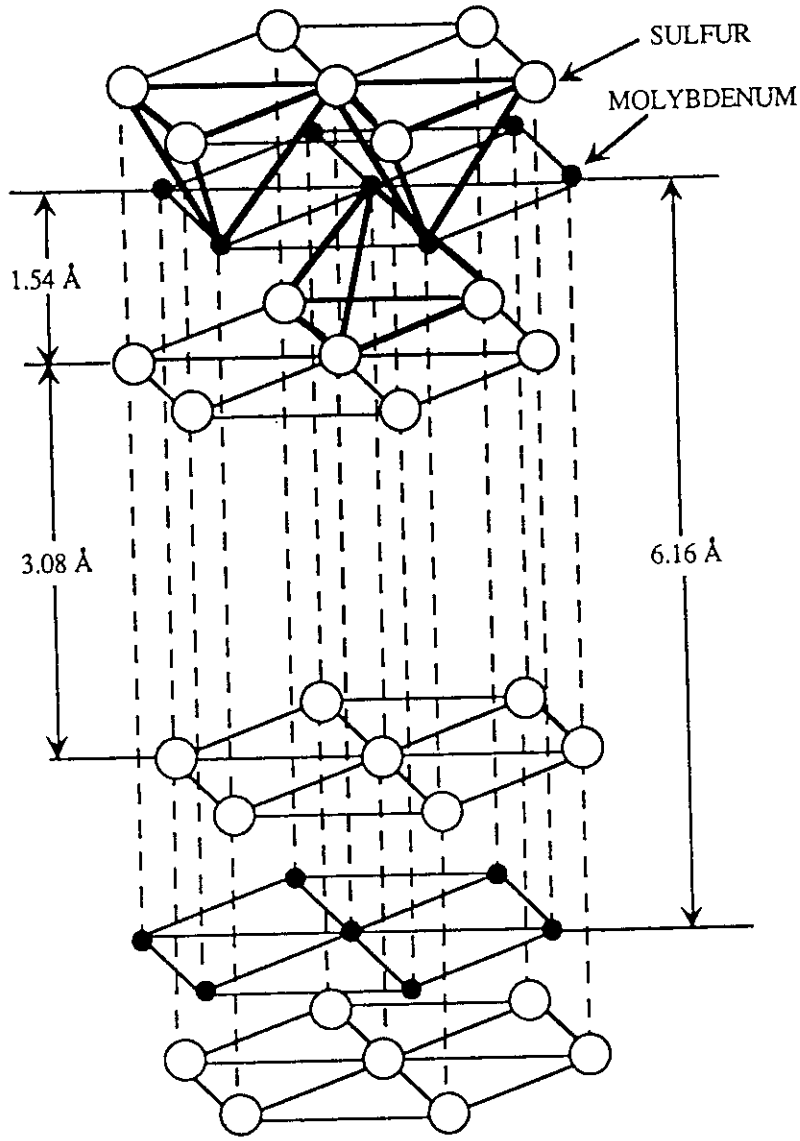

Figure 18. Layer lattice structure of molybdenum disulfide, MoS_2.

between atoms within the lamellae. As a result, these lamellar crystals easily shear along the van der Waals gap between the lamellae. These structures are comparable to a stack of paper sheets which can be easily spread horizontally but can support high loads applied perpendicularly to the page surface.

Various dichalcogenides, namely MoS_2, WS_2, NbS_2, $MoSe_2$, $TaSe_2$ and $MoTe_2$ have been deposited by sputtering to produce solid lubricant films [58]; only MoS_2, WS_2, $MoSe_2$ and $NbSe_2$ are consistently good lubricants under the experimental

conditions investigated. The most widely used material of this group is MoS_2. The preparation of adherent MoS_2 thin films by radio frequency sputtering from a MoS_2 target as well as the structure and friction properties of these films have been thoroughly investigated by NASA scientists. A review of advances in solid lubrication with sputter-deposited MoS_2 films was published recently by Spalvins [59].

Excellent adherence of sputter-deposited MoS_2 films caused by strong metal-sulfur bonds can be obtained on 304 stainless steel substrates cleaned by appropriate surface treatments prior to the sputter-deposition of films. The lubricating properties of adherent films depends strongly on the stoichiometry of the deposited material, morphology of films, grain size and their related distributions in the films. The substrate temperature affects the nucleation and growth characteristics of sputter-deposited MoS_2 films. As a result, the microstructure (crystallite size) and friction coefficient of these films are strongly dependent on the substrate temperature (Fig.19). Ultrathin films of 200 to 500 Å in thickness with amorphous structure (crystallite size of about 10 Å) have been deposited on substrates at cryogenic temperatures (- 195°C). These films with no crystallinity are abrasive and exhibit a friction coefficient of 0.4 in vacuum or air. For ultrathin films deposited on substrates at ambient or elevated temperatures (320°C), the crystallite size is in the range 110-140 Å, the lubricating properties are excellent and friction coefficient values as low as 0.04 are obtained in vacuum, dry air or argon atmosphere. Electron transmission micrographs of these crystallized MoS_2 lubricant

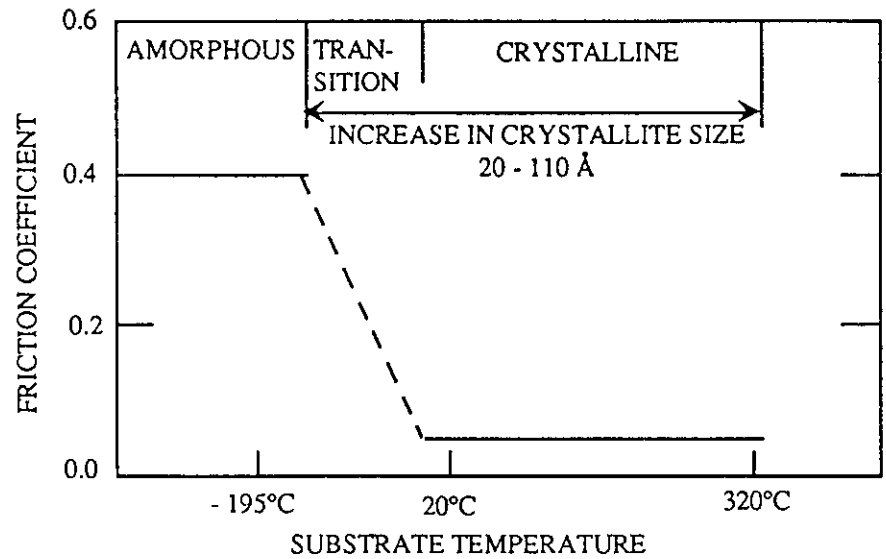

Figure 19. Effect of the substrate temperature on MoS_2 friction coefficient and microstructure of films [64].

films exhibits a characteristic ridge formation pattern [59]. Mixed crystalline-amorphous phases can be formed at substrate temperatures lower than 10°C. The friction coefficient of these films rises progressively up to 0.4 as the relative amount of amorphous phase

increases. As the thickness of MoS_2 films exceeds 800 Å, the ridge structure transforms into an equiaxed dense transition zone before formation of a columnar-fiber-like structural network observed by scanning electron microscopy and schematically presented in Fig.20. Basically, the equiaxed zone of 2000 Å in maximum thickness is pore free and has a densely packed structure. On top of this zone, the columnar-fiber structure consists of vertical columns of about 2500 Å in diameter perpendicular to the substrate surface and separated by open voided boundaries of a few hundred Å in width.

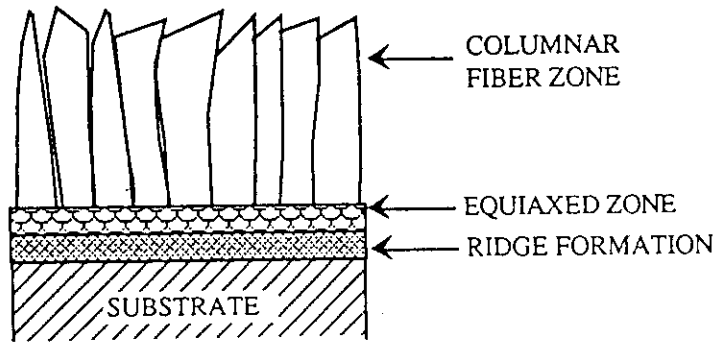

Figure 20. Morphology of sputtered MoS_2 films [59].

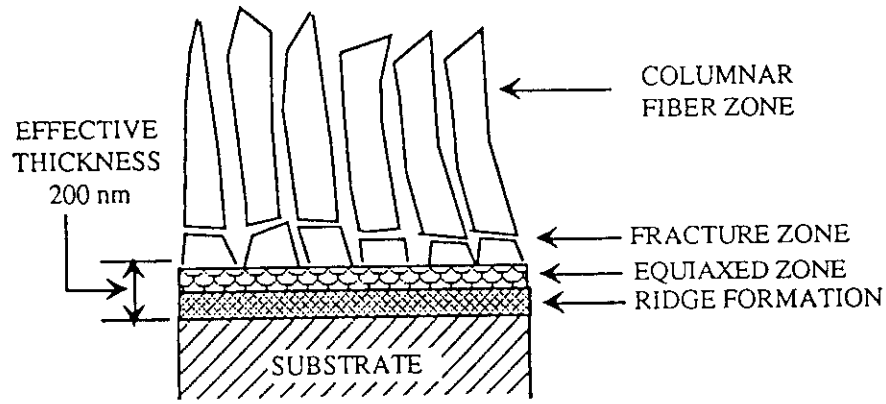

Figure 21. Fracture and morphology of sputtered MoS_2 films during sliding [59].

Lubricating properties of sputter-deposited MoS_2 films of a thickness in the range 0.7-2 μm were studied and reported in the literature. The effective film thickness required for precision bearing lubrication was recently established in terms of the morphology of films during pin-on-disk tribological tests [60]. Films of 1.2 μm thick have a tendency to break within the columnar-fiber-like zone above the equiaxed zone (Fig.21). The remaining lubricating film adherent to the substrate is between 0.18 and 0.22 μm thick. Wear debris corresponding to broken columns can impair the lubrication cycle especially in high-precision bearings with close tolerances.

To strengthen the structure of the columnar zone and to increase the thickness of the effective lubricating film, gold, nickel, chromium, cobalt or tantalum were co-sputter-deposited with MoS_2 [61,62]. These MoS_2-based lubricant films display smoother friction and increased endurance life. A near linear increase in endurance life of MoS_2:Ni films is observed as the film thickness increases up to 8 μm [63].

The friction coefficient of sputter-deposited MoS_2 films is strongly dependent on the bias voltage applied to the substrate [64], i.e., the lubricating properties are lost as the substrate is biased to - 350 V during sputter-deposition (Fig.22). In fact, the sulfur concentration in the deposited material is considerably affected by the bias voltage. A large depletion of sulfur is observed in films sputter-deposited on biased substrates.

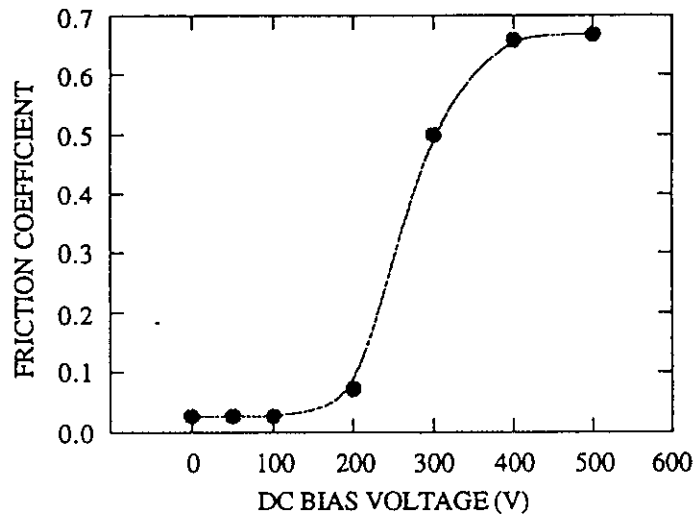

Figure 22. Friction coefficient of MoS_2 films versus negative dc bias voltage applied to 440C steel substrates; the tribological tests were performed under a load of 250 g at a sliding velocity of 40 rev min^{-1} with a rider made of 440C steel. The friction coefficient was about 0.65 with the 440C steel rider sliding directly against a 440C steel disk [64].

The endurance life and friction coefficient of sputter-deposited MoS_2 films are very sensitive to the gas environment. For MoS_2 films sliding against a nickel rider, the friction coefficient increases from 0.04 in vacuum to 0.15 in air (Fig.23). Low oxidation of MoS_2 films by oxygen and water vapor in air leads to failures and rapid increase in friction coefficient (Fig.24). The stability of lubricating films is improved when polytetrafluoroethylene (PTFE) is incorporated in the deposited material. For instance, in moist air, the friction coefficient of co-sputter-deposited MoS_2:PTFE films is 0.1 instead of 0.3 for pure MoS_2 films and the endurance life is 10 times longer than that of conventionally sputter-deposited MoS_2 films [65].

Furthermore, the endurance life of sputter-deposited MoS_2 films in vacuum can be considerably improved when a hard coating such as sputter-deposited Cr_3Si_2 films is interposed between the substrate and the lubricating film [51]. With 0.2-μm-thick MoS_2

films sputter-deposited on the raceways and the cages of bearings, a reasonable life time of about 200 h is obtained. For bearings with an intermediate 0.1-μm-thick Cr_3Si_2 film sputter-deposited on the raceway, tests can be performed for 1000 h without failure.

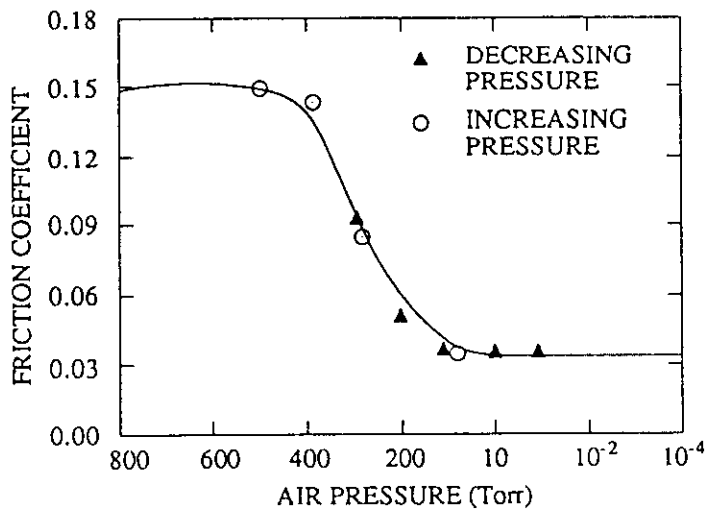

Figure 23. Friction coefficient of MoS_2 films sputter-deposited on nickel disks versus air pressure; the tribological tests were performed at room temperature under a load of 250 g at a sliding velocity of 40 rev min^{-1} with a nickel rider and a nickel disk [51].

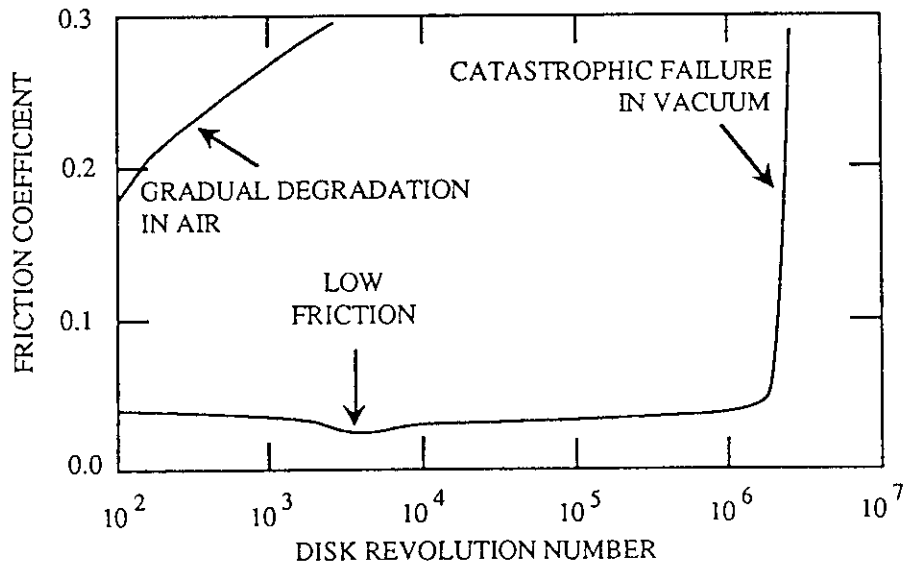

Figure 24. Failure modes of sputter-deposited MoS_2 films during sliding motion in air and in vacuum [51].

The lubricating properties of sputter-deposited MoS_2 or WS_2 films can be improved after ionic bombardment of films. Bombardment of WS_2 films of thickness higher than 1 μm by high energy Ar ions (50 keV at 5 x 10^{15} ions cm^{-2}) results in a decrease in friction coefficient from 0.03 to 0.01 in vacuum while the endurance life of these ion-bombarded WS_2 films in both air and vacuum increases by a factor of 2 [66]. This improvement in friction properties is attributed to the amorphization and recrystallization of films. Ion bombardment of sputter-deposited films can result in fully dense structure and film-substrate interface mixing. For instance, improved lubricant films are produced if sputter-deposited MoS_2 films of 500 Å thick are bombarded with Ar, Kr or Xe ions of 400 keV before sputter-deposition of an additional MoS_2 films of 2 μm; the adherence of the resulting film is doubled and the endurance life increases by about 50 % compared to conventional sputter-deposited MoS_2 films of similar thickness [67]. Moreover, the friction coefficient of ion beam amorphized MoS_2 films deposited by sputtering is about 0.04. This value is in agreement with those reported for crystallized MoS_2 films but disagrees with the friction coefficient of 0.4 measured for "amorphous" films sputter-deposited on substrates at cryogenic temperatures [59]. These results suggest that the poor lubricating properties of films sputter-deposited at very low temperatures would be attributed to the effect of deposition conditions and chemical composition of films rather than to the lack of crystallinity. Further investigations are necessary for a better understanding of the friction behavior of non-crystalline MoS_2 films sputter-deposited on cooled substrates.

4.3. CARBON-BASED COMPOUNDS

Polymers and polymer composites are used as solid lubricants in particular for lubrication of moving mechanical assemblies operating in vacuum [68]. To date, polytetrafluoroethylene (PTFE) has been the polymer used the most in vacuum. This material also exhibits suitable lubricating properties in the presence of absorbed vapors; however, it has a tendency to cold flow under a load and a binder is required for minimization of the plowing action. Furthermore, some polyimides are excellent lubricants in vacuum. The lubricating properties of these polymers are very affected by water vapor absorption which inhibits molecular shear. Polymer composites consist of mixture of polymer (PTFE, polyimide) with other materials (glass fiber, MoS_2) added to increase load-carrying capacity, to lower the friction coefficient, to reduce wear rate and to increase thermal conductivity [68].

Graphite fluoride, $(CF_x)_n$, is a relatively new solid lubricant with a lamellar crystal structure similar to a layer lattice intercalation compound of graphite [69]. This material is prepared by the direct reaction of graphite with fluorine at controlled temperature and pressure. Burnished films of graphite fluoride powder have an excellent potential as solid lubricants for use at temperatures up to 400°C. The friction coefficient is comparable to that of MoS_2 while the endurance life is superior or similar to that of MoS_2. The lubricating properties of this carbon-based compound is not affected by changes of the fluorine to carbon ratio in the range $(CF_{0.7})_n$ to $CF_{1.12})_n$. Fluorocarbon polymer films with similar composition deposited by radio frequency sputtering of a PTFE target exhibit lubricating properties similar to those of PTFE [70].

Besides polymer materials, hydrogenated or unhydrogenated diamond-like carbon (DLC) films produced by sputtering or plasma-enhanced CVD techniques possess

excellent lubricating properties [54,71]. These amorphous films can combine properties of solid lubricating graphite structure and hard diamond crystal structure, i.e., extreme hardness, chemical inertness, high thermal conductivity and optical transparency without the crystalline structure of diamond. The excellent tribological properties of amorphous carbon films reported by Miyake [72] can be analyzed in detail to illustrate the potential of plasma-enhanced CVD techniques in preparation of solid lubricant films which were tested in vacuum and in air with a reciprocating sliding tester [73].

4.3.1. *Diamond-Like Carbon Films Produced by Plasma-Enhanced Chemical Vapor Deposition*

The deposition system used to prepare these diamond-like carbon films is equipped with a thermal cathode (tungsten filament) emitting electrons by thermoionic effect. These energetic electrons collide with either ethylene, C_2H_4, or methane, CH_4, molecules to produce the plasma. Ions are extracted from the plasma and condensed on the substrate biased to an appropriate d.c. voltage.

Two types of amorphous carbon films can be obtained depending upon deposition conditions [74]. Carbon films with a relative low hydrogen content, named DLC films, are produced from ethylene at a high substrate voltage (- 3.5 kV) and a low gas pressure (0.7 Pa). A second type of films with the hydrogen content about four times higher can be deposited from methane at a low substrate voltage (- 0.3 kV) and a high gas pressure (130 Pa); these films consist of amorphous hydrogenated carbon (a-C:H films). According to reflection electron and x-ray diffraction patterns, the DLC films are composed of a mixture of diamond and graphite phases.

The friction coefficient of DLC films is as low as 0.15 in air because of the lubricating effect of the graphite phase (Fig.25(1)); by contrast, the friction coefficient in vacuum increases up to 0.3-0.4 after only one or two cycles. This friction behavior is similar to that of graphite [18]. The reverse situation can be observed with a-C:H films after 10 cycles (Fig.25(2)). In vacuum, the friction coefficient becomes nearly equal to 0.01 between 50 and 200 cycles and then increases up to 0.35 at 2000 cycles. The a-C:H films, wear debris and material transferred on the rider were analyzed by infrared spectroscopy to determine the lubrication mechanism involved in these tribological tests. The extremely low friction coefficient of 0.01 may result from the formation of oriented hydrocarbons on the rider surface; hydrocarbons strongly adhere to the rider surface even in vacuum [75].

4.3.2. *Amorphous Hydrogenated Silicon-Carbon Films Produced by Plasma-Enhanced Chemical Vapor Deposition*

Amorphous hydrogenated silicon-carbon films (a-SiC:H films) can be prepared by electron cyclotron resonance (ECR) plasma-enhanced CVD techniques [76]. These films with various concentrations of carbon and silicon can be produced by varying the ratio of the ethylene to silane flow rates. The silicon incorporation in carbon films results in improved adherence of films to single crystal silicon and stainless steel substrates. These amorphous SiC:H films contain considerable amounts of hydrogen and can be converted into films with a crystal-like SiC structure by annealing above 600°C.

The friction characteristics of unannealed SiC:H films in vacuum depend on the silicon content (Fig.26). The films containing 10 at% of silicon display an extremely low friction coefficient of 0.01 after an initial stage of 100 to 300 cycles; the minimum

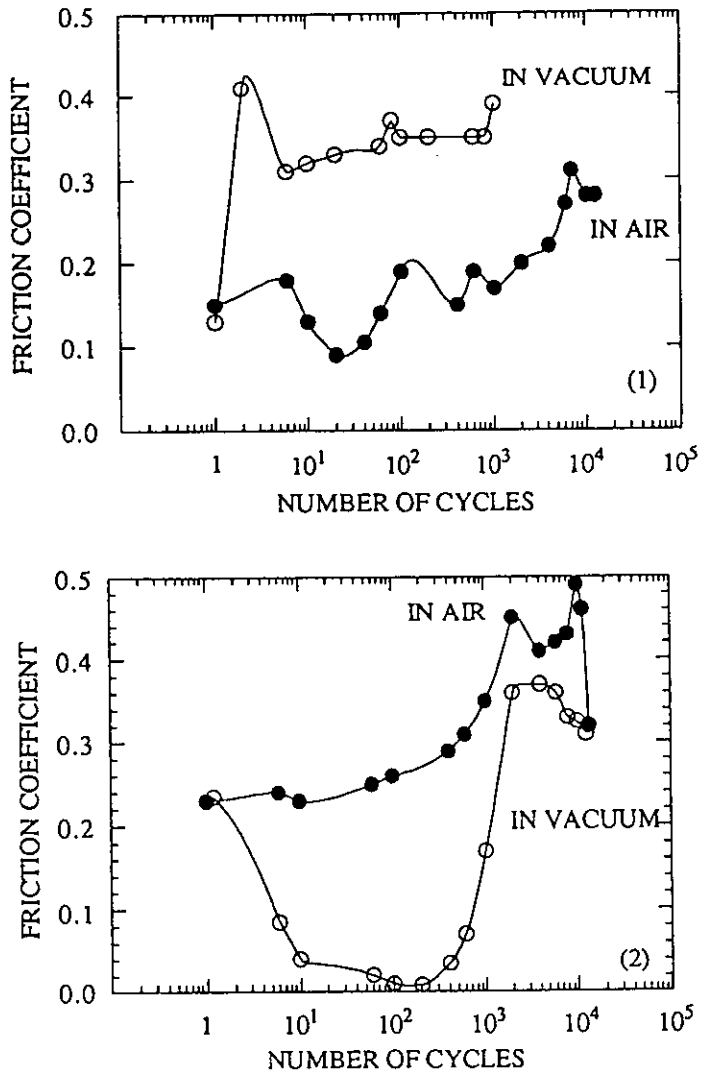

Figure 25. Friction coefficients of : (1) DLC films, and (2) a-C:H films in air and in vacuum ($P = 10^{-5}$ Pa); the load and the sliding velocity were 4.9 N and 12 cm s^{-1}, respectively [72].

friction coefficient value of 0.007 is obtained at 300 cycles. In the case of pure a-C:H films produced by ECR plasma-enhanced CVD from ethylene, the friction coefficient increases sharply after about 10 cycles and never is as low as that of a-C:H films produced by plasma-enhanced CVD from methane. In fact the a-C:H films prepared by ECR plasma-enhanced CVD are not sufficiently adherent to substrates and peel off. Finally, the friction coefficient of silicon-rich carbon films never is less than 0.2 or 0.3.

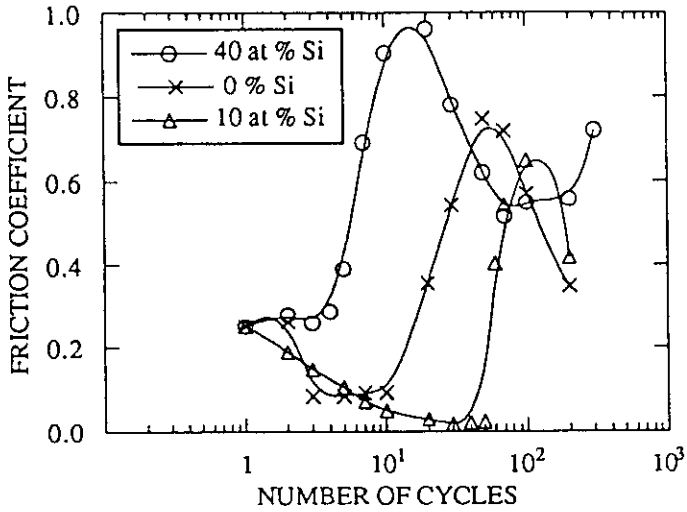

Figure 26. Friction coefficient of amorphous SiC:H films in vacuum (P = 10^{-5} Pa); the load and the sliding velocity were 4.9 N and 12 cm s^{-1}, respectively [72].

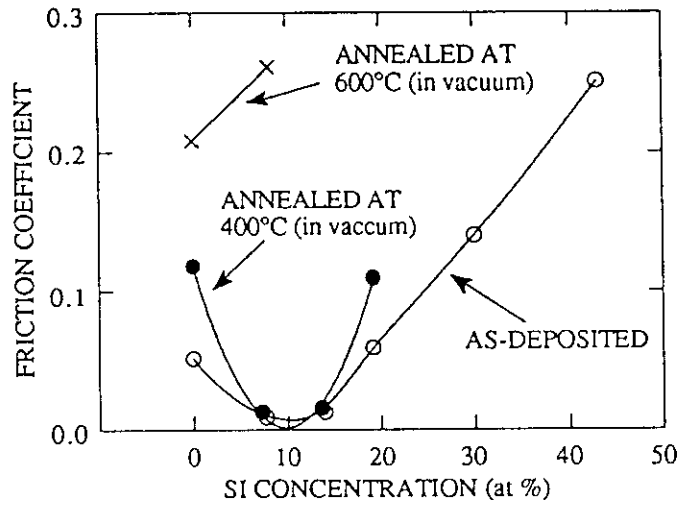

Figure 27. Minimum values of the friction coefficient of as-deposited and annealed SiC:H films in vacuum (P = 10^{-5} Pa); the load and the sliding velocity were 4.9 N and 12 cm s^{-1}, respectively [72].

The minimum friction coefficient values of amorphous SiC:H films in vacuum depend on the silicon concentration and annealing temperature (Fig.27). The as-deposited amorphous SiC:H films with 7 to 13 at% of silicon exhibit extremely low friction coefficients in vacuum. A similar behavior is observed for films annealed at 400°C.

After annealing at 600°C, the friction coefficient of films is higher than 0.2. In fact, during annealing treatment at 600°C, hydrogen atoms are eliminated and the crystalline SiC phase forms. As a result, the extremely low friction coefficients are probably caused by the effect of hydrogen incorporated in the amorphous films.

4.4. SOFT METALS

Soft metals as gold, silver, lead, tin and indium easily undergo plastic deformation. Effective lubrication with soft metal films can be achieved with optimized film thickness and excellent film-substrate adherence. Ion-assisted deposition (IAD) techniques such as ion plating and sputtering are very attractive to produce adherent soft metal films with graded film-substrate interface, i.e., with a gradual composition at the interface. Ion-plated lead films are particularly effective lubricant films in spacecraft bearings employed in solar array drive mechanisms. In addition, with IAD techniques various properties of films such as density, internal stresses, morphology, microstructure can be modified and significantly improved. As a result, lubricating properties of films can be favorably affected.

4.4.1. *Ion-Plated Soft Metals*

The ion plating technique is based on thermal evaporation of metal to be deposited on substrates. The metal vapor passes through an argon glow discharge before condensation on the substrates. Typically, 1 % of the vaporized metal atoms are ionized before deposition on substrates. The glow discharge is produced by biasing the substrates to a negative voltage (- 2 to - 5 kV) in argon atmosphere (0.7 to 30 Pa). The substrates experience high energy ion bombardment resulting in ion etching of impurities present on the substrate surface. This cleaning effect is very favorable for improving adherence and for providing gradual interface composition. The continuous ion bombardment leads to films with fine uniform grain structure and high packing density.

The friction coefficient of ion-plated soft metal films is minimum for a critical film thickness as illustrated in Fig.28 for Pb and Au films [77]. The tribological properties of these gold films are better than those of metal films produced by conventional thermal evaporation (Fig.29). The ion-plated gold films exhibit improved endurance life, lower friction coefficient and lack of catastrophic failure [59]. The increased endurance life is caused by a stronger adherence than that of vapor-deposited gold films. The reduced friction coefficient is provided by more dense structure with small crystallite size than in vapor-deposited films.

4.4.2. *Sputter-Deposited Silver Films*

Silver is a soft metal with low shear strength, high thermal conductivity, excellent chemical inertness and moderately high melting point (961°C); these properties are desirable for solid lubricant films operating in hostile environments (high temperatures in oxidizing atmosphere). Bombardment of growing films by low energy ions can be achieved during deposition of films by cathode sputtering. In addition, the sputtered atoms arrive at the substrate surface with substantial mean energy compared with evaporated species. As a result, during sputter-deposition of films, the surface mobility of adatoms is enhanced and atomic or ion peening phenomena [78] can be favored as if the films were deposited by ion plating.

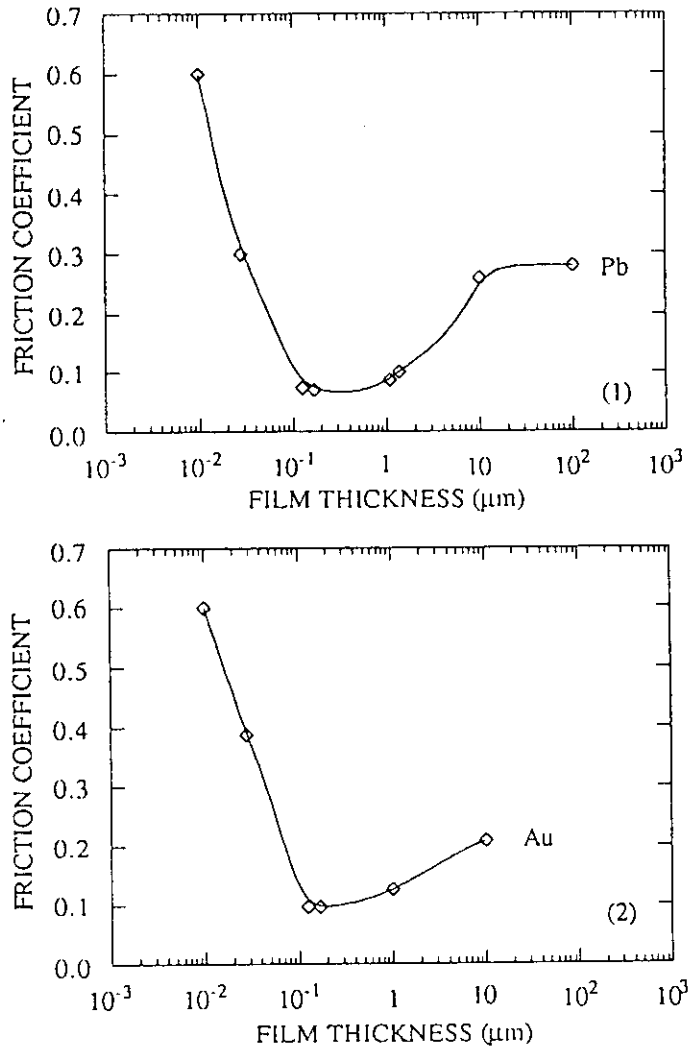

Figure 28. Friction coefficient versus film thikness in vacuum for : (1) ion-plated lead films, and (2) ion-plated gold films on 440C steel substrates [59].

Recently, silver films have been prepared by radio frequency sputtering and tribological properties of films deposited on superalloy substrates were investigated at room temperature and at 500°C [79-82]. Under the sputter-deposition conditions used, 0.4-to-20-μm-thick silver films exhibit a crystallographic structure preferentially oriented in the (111) direction with crystallite size of 60 to 150 nm. The morphological structure of films examined by scanning electron microscopy is found to be fully dense. The compressive residual stresses in these sputter-deposited silver films are as low as -0.05 GPa.

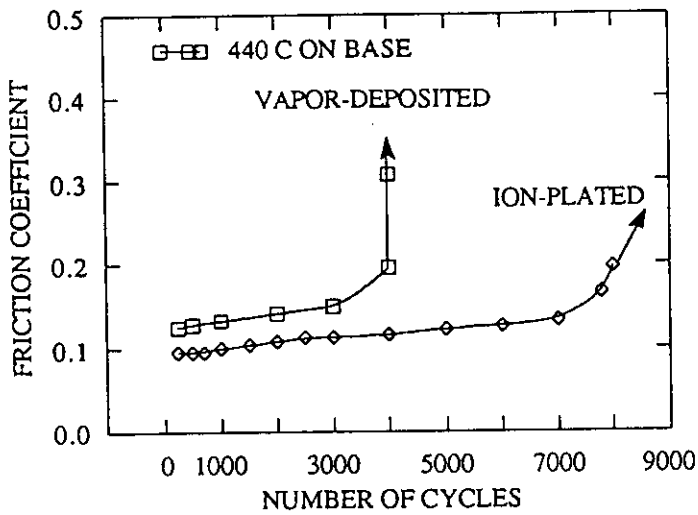

Figure 29. Friction coefficient versus number of cycles in vacuum for 2000 Å thick ion-plated and vapor-deposited gold films on 440C steel substrates [59].

The tribological tests were conducted in a standard ball-on-disk apparatus; the 10-mm-thick alacrite disk specimen of 45 mm in diameter was rotated about the vertical axis and the alumina ball specimen of 8 mm in diameter with an average surface roughness, R_a, of about 0.03 μm was held firmly in a fixed position. The disk specimens with a surface finish, R_a, of 0.2-0.3 μm were manufactured from a superalloy (alacrite) constituted of cobalt (53.9 at%), chromium (25 at%), nickel (11.8 at%), tungsten (4.7 at%), iron (2.4 at%), manganese (1.2 at%) and molybdenum (0.3 at%). The hardness of these superalloy substrates determined by the Brinell technique was 388 MPa. The diameter of the disk wear track was varied from 21 to 28 mm, i.e., the average distance covered per cycle was 7.7 cm. The tests were run in ambient air, at room temperature and 500°C, with a sliding velocity of 0.02 m/s, under loads of 1, 2.9 and 9.8 N corresponding to an initial Hertz pressure of 270, 390 and 590 MPa, respectively. The relative air humidity was in the range 40-60 % at room temperature. Friction and load forces were recorded for the test duration which was varied from 5 to 100 h. These test conditions were selected to be realistic for lubrication of sliding contacts by sputter-deposited silver films in mechanical components operating at elevated temperatures.

The friction coefficient of various coated and uncoated alacrite disks sliding against alumina balls at room temperature was measured as a function of the number of cycles. The baseline data reported in Fig.30 correspond to tribological tests performed with unlubricated alacrite disks-alumina ball test pairs under a load of 1 N. The tribological tests were performed with alacrite disks coated with 1.7-μm-thick silver films under loads of 9.8, 2.9 and 1 N at room temperature for 5000 cycles, i.e., an average sliding distance of 385 m. The initial value of the friction coefficient is equal to 0.25 independently of the load value (Figs.30 and 31). Under loads of 9.8 and 2.9 N, the

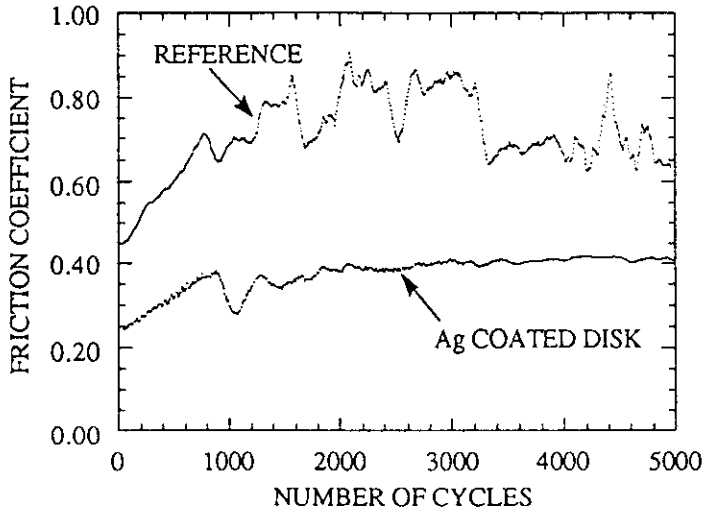

Figure 30. Friction coefficient versus number of cycles for : unlubricated alacrite disk specimen under a load of 1 N (reference) and an alacrite disk specimen covered with a 1.7-μm-thick silver film under a load of 9.8 N [82].

friction coefficient rises progressively up to 0.35-0.40 during the 1000 first cycles before stabilization. The initial increase in friction coefficient is not observed under a load of 1 N; in fact, the friction coefficient value is stable at 0.25 during the 1500 to 2000 first cycles and increases very progressively for reaching 0.35-0.40 at the end of

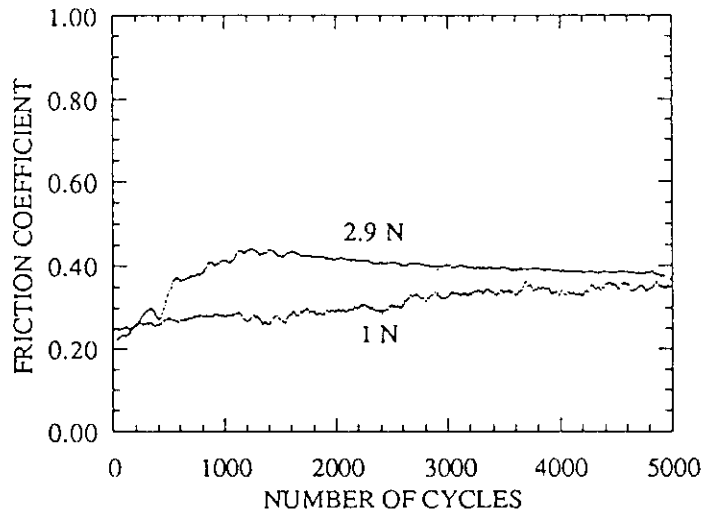

Figure 31. Friction coefficient versus number of cycles for alacrite disk specimens coated with a 1.7-μm-thick silver film under various loads [82].

the tests (Fig.31). These results demonstrate that the friction coefficient of alacrite disks coated with 1.7-μm-thick silver films increases very slightly as the load and number of cycles increase in the range 1 to 9.8 N and between 1000 and 5000 cycles, respectively. Under the tribological test conditions investigated, the average friction coefficient value of about 0.35 can be considered as a relevant data, characteristic of these test specimens.

The friction coefficient of 4.8-μm-thick silver films deposited on alacrite disks was also investigated as a function of the number of cycles at room temperature under a load of 1 N (Fig.32); the test specimens were previously annealed at 500°C for 4 h in air. At the initial stage of the tribological tests, the friction coefficient is 0.35, then decreases and remains stable at about 0.27 between 5000 and 60 000 cycles. Beyond this number of cycles, the friction coefficient value increases progressively up to 0.32 for 90 000 cycles, i.e., for an average sliding distance of 7 km. The average friction coefficient value of 0.30 over this large number of cycles can be considered as a characteristic feature of these silver films.

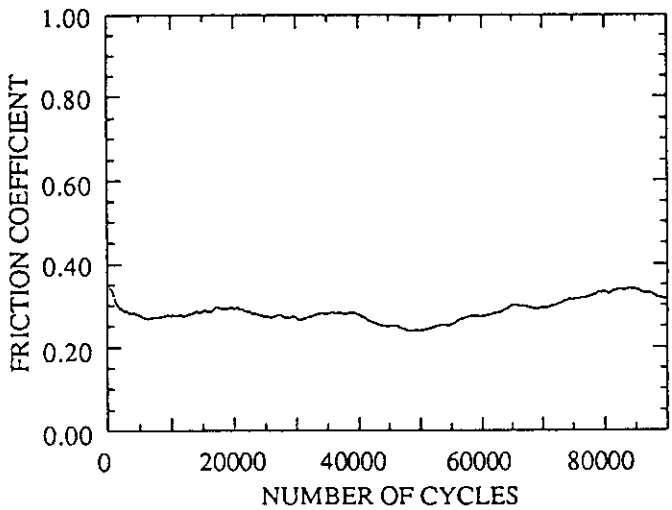

Figure 32. Friction coefficient versus number of cycles for an alacrite disk specimen coated with a 4.8-μm-thick silver film under a load of 1 N [82].

In another series of experiments, the friction coefficient of silver coated alacrite disks sliding against alumina balls was determined as a function of the number of cycles under a load of 1 N at room temperature and 500°C with silver films of various thicknesses. After an initial stage corresponding to about 1000 cycles, the variation of the friction coefficient up to 5000 cycles is rather small (Figs.33 to 36). The disks covered with silver films thinner than about 2 μm exhibit a friction coefficient lower at room temperature than at 500°C; the reverse situation prevails when the film thickness is greater than 2 μm. The average value of the friction coefficient depended on both the film thickness and temperature (Fig.37). For silver films of 0.4 μm in thickness, the average friction coefficient is relatively high, namely 0.40 and 0.30 at room temperature and 500°C, respectively. The average value decreases sharply with increasing film

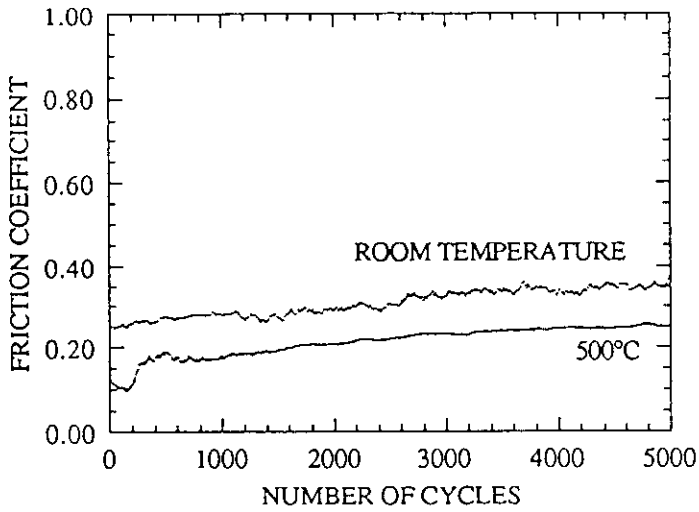

Figure 33. Friction coefficient versus number of cycles for alacrite disk specimens coated with a 1.3-μm-thick silver film under a load of 1 N [82].

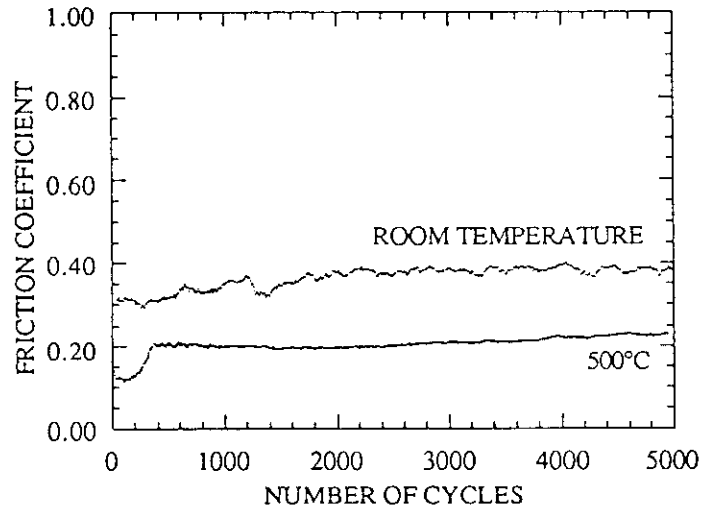

Figure 34. Friction coefficient versus number of cycles for alacrite disk specimens coated with a 1.7-μm-thick silver film under a load of 1 N [82].

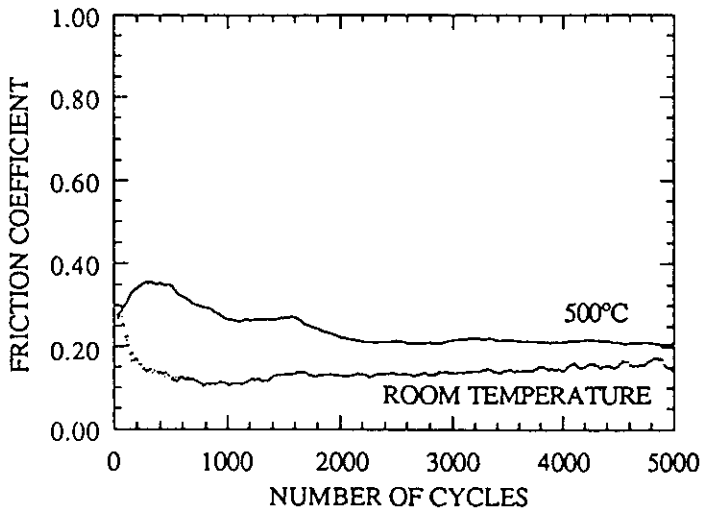

Figure 35. Friction coefficient versus number of cycles for alacrite disk specimens coated with a 4.8-μm-thick silver film under a load of 1 N [82].

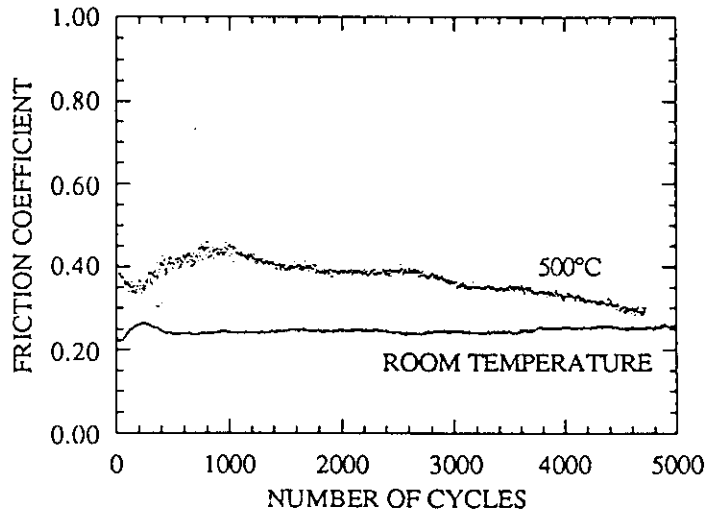

Figure 36. Friction coefficient versus number of cycles for alacrite disk specimens coated with a 20-μm-thick silver film under a load of 1 N [82].

thickness and is equal to 0.20 for 4.8-μm-thick silver films at room temperature and for 1-to-2-μm-thick silver films at 500°C. The friction coefficient of thicker silver films increases progressively with increasing film thickness; for example, alacrite disks coated with silver films of 20 μm in thickness possess an average friction coefficient of 0.20 and 0.40 at room temperature and 500°C, respectively. In addition, as displayed by the

diagram given in Fig.37, the critical thickness of silver films providing the minimum value of the friction coefficient is dependent on the test temperature.

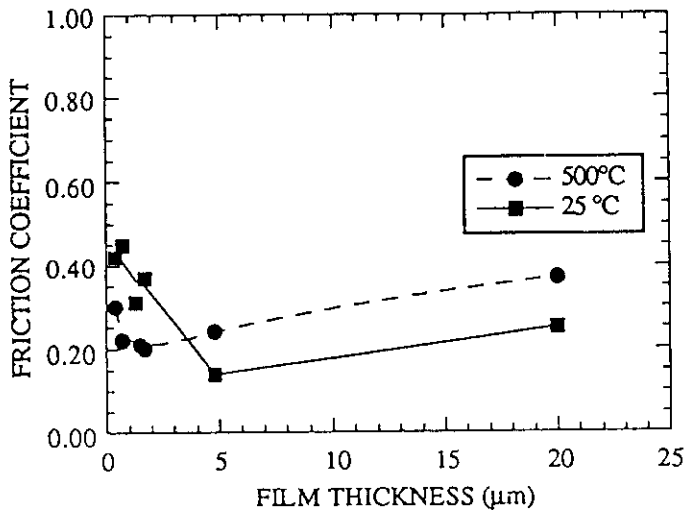

Figure 37. Average friction coefficient versus thickness of silver films under a load of 1 N [82].

To establish a relationship between the film thickness and the friction coefficient, a theoretical model was proposed by Halling [34,35]; the friction coefficient, μ, predicted from this model is given by the following expression :

$$\mu = \frac{\mu_{t\to 0}\,\overline{H}\,\overline{\lambda} + \left[\exp\left(\frac{t}{\sigma}\right) - 1 - \frac{t}{\sigma}\right]\mu_{t\to\infty}}{\overline{H}\,\overline{\lambda} + \left[1 + (\overline{H} - 1)\exp\left(-\frac{c\,t}{\beta}\right)\right]\left[\exp\left(\frac{t}{\sigma}\right) - 1 - \frac{t}{\sigma}\right]} \qquad (17)$$

where t is the film thickness, σ the standard deviation value of the distribution of surface asperities, β the radius of the asperities and c a constant. According to Eq.(17), when the film thickness tends to be zero, the friction coefficient, μ, will be equal to $\mu_{t\to 0}$, and for very thick films, the friction coefficient will be equal to $\mu_{t\to\infty}$. The values of $\mu_{t\to 0}$ and $\mu_{t\to\infty}$ can be deduced from the experimental results given in Figs.30 and 37, i.e., for tribological tests at room temperature $\mu_{t\to 0}$ = 0.70 and $\mu_{t\to\infty}$ = 0.25. The term $\overline{\lambda}$ given by the ratio, λ_1/λ_2, may be estimated depending on the anticipated mode of deformation of the film and substrate materials; a soft film would be deformed plastically with λ_2 = 2 while the harder substrate might behave elastically with λ_1 = 1 [34,35]. For silver films deposited on alacrite substrates, the reasonable value of $\overline{\lambda}$ would be equal to 0.5.

Furthermore, the expression defining $\overline{H}$ is the ratio, H_1/H_2, where H_1 and H_2 are the hardness of the substrate and film materials, respectively. The effective hardness, H_e, i.e., the hardness of the film coated substrate can be calculated from the following empirical expression [34,35] :

$$H_e = H_2 + (H_1 - H_2) \exp\left(-\frac{c\,t}{\beta}\right) \tag{18}$$

The hardness of the film material, H_2, i.e., the hardness of bulk silver is equal to 600 MPa [84]. In addition, the hardness values of silver coated alacrite disks or the effective hardness, H_e, were measured by the Brinell technique at room temperature under experimental conditions (alumina ball of 8 mm in diameter and load of 1 N) similar to those used for tribological tests. The experimental values of H_e measured at room temperature and the value of H_2 = 600 MPa can be introduced in Eq.(18) to plot (H_e - H_2) or (H_e - 600) versus film thickness. The value of the coefficient c/β deduced from

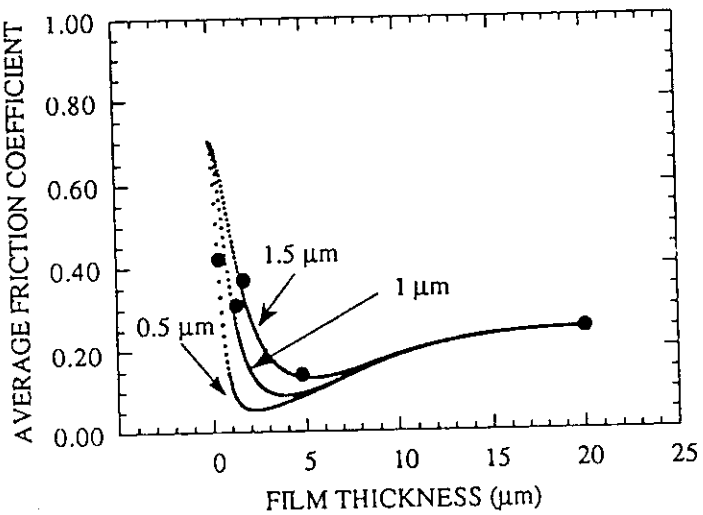

Figure 38. Average friction coefficient versus thickness of silver films; the theoretical curves correspond to a standard deviation, σ, of the asperity distribution of : 1.5 µm, 1 µm and 0.5 µm [82].

this graph by fitting the data points with Eq.(18) is equal to 0.32. As a result, the expression of the friction coefficient given by Eq.(17) can be written as follows :

$$\mu = \frac{3.5 + 0.25\left[\exp\left(\frac{t}{\sigma}\right) - 1 - \frac{t}{\sigma}\right]}{5\left[1 + 9\exp(-0.32\,t)\right]\left[\exp\left(\frac{t}{\sigma}\right) - 1 - \frac{t}{\sigma}\right]} \tag{19}$$

In fact, the friction coefficient can be plotted versus film thickness for various values of σ, for example, for σ equal to 1.5, 1 and 0.5. As illustrated in Fig.38, the data points corresponding to the friction coefficient obtained from silver films of various thicknesses for tribological tests performed at room temperature are in good concordance with the theoretical curves.

4.5. INORGANIC MATERIALS

Solid lubrication needs at high temperatures in oxidizing atmosphere have arisen for new technology especially for supersonic and future hypersonic aircraft. Much research has been performed on various soft oxides and with fluorides of alkali metals and alkaline earth metals [50]. The alkaline earth metal fluorides exhibit a fragile-ductile transition at high temperatures, in particular CaF_2 crystals show appreciable ductility above 400°C [84,85]. Accordingly, these materials may serve as solid lubricants at high temperatures.

4.5.1. *Sputter-Deposited Calcium Fluoride Films*

Films of calcium fluoride, CaF_x with x = 1.85, were produced by RF diode sputtering of a hot-pressed CaF_2 target. The tribological tests of CaF_x coated alacrite disks were performed under experimental conditions similar to those described for sputter-deposited silver films [86,87].

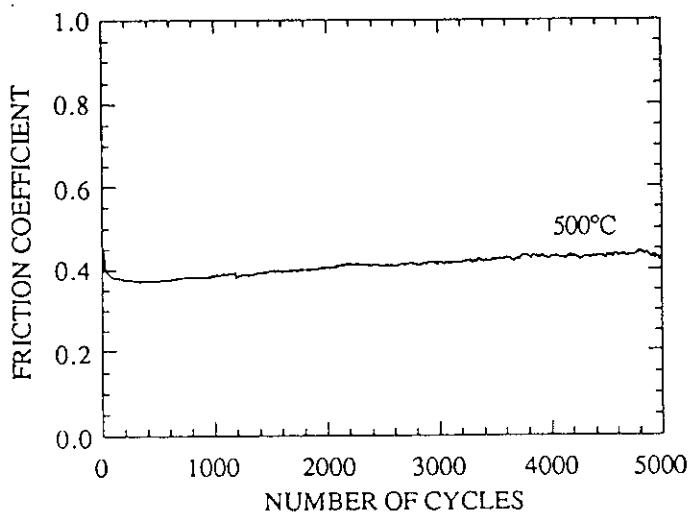

Figure 39. Friction coefficient versus number of cycles for 1.2-μm-thick CaF_x films under a load of 1 N in air at 500°C [87].

The friction coefficient of 1.2-μm-thick CaF_x coated alacrite disks sliding against an alumina ball in air at 500°C is found to be essentially constant and equal to about 0.4 for 5000 cycles (Fig.39). The depth of wear tracks was observed to be less than the film thickness after 5000 cycles excepted for CaF_x films of 0.2 μm in thickness. Nevertheless, SEM examinations of wear tracks reveal that the alacrite substrate can

appear locally in the bottom of the wear tracks. In addition, after tribological tests, the alumina balls are found to be covered with a layer of CaF_x originating from the wear of the CaF_x films deposited on the tribological disks. Furthermore, no wear scar is detected in the wear tracks by SEM examinations. The bottom of wear tracks is essentially flat excepted in the zones where the CaF_x film is stripped and the alacrite substrate can be detected.

The friction coefficient of CaF_x coated alacrite disks was also investigated as a function of the film thickness in air at 500°C under a load of 1 N. The average friction coefficient after 5000 cycles is relatively high (0.6 to 0.7) for the thinnest films and decreases progressively down to 0.4 as the film thickness increases (Fig.40). The critical thickness of CaF_x films corresponding to this minimum friction coefficient is about 1 μm. The friction coefficient of alacrite disks covered with CaF_x films thicker than 1 μm was essentially constant, i.e., in the range 0.40-0.45.

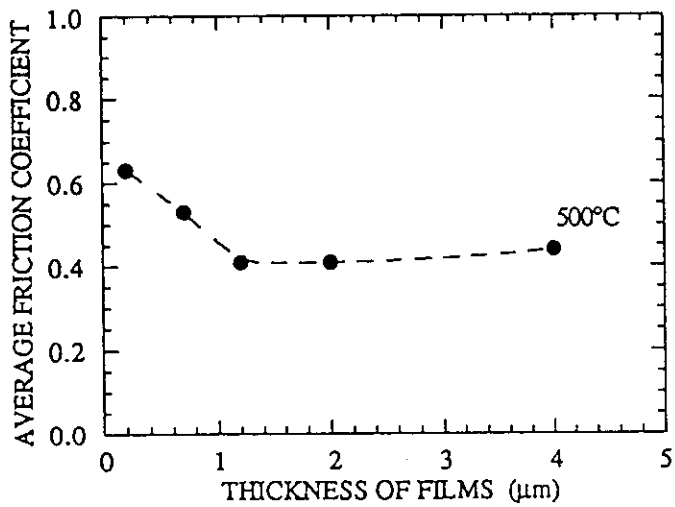

Figure 40. Average friction coefficient versus thickness of CaF_x films under a load of 1 N in air [87].

4.5.2. *Sputter-Deposited Silver/Calcium Fluoride Multilayer Films*

The friction properties of alacrite disks covered with Ag/CaF_x multilayer films were determined at room temperature and 500°C to examine the synergetic effects of lubricant films susceptible to step in tribological tests. The friction coefficient of Ag/CaF_x coated disks is found to be approximately constant for 5000 cycles at room temperature as well as at 500°C excepted for the 100 first cycles (Fig.41). The friction coefficient is similar to that of silver coated disks at room temperature, i.e., the friction properties of silver are not affected by the CaF_x films interposed between silver films. At 500°C, the friction coefficient is relatively high for 100 to 200 cycles. The average friction coefficient for samples with various thicknesses of lubricant films lies between 0.34 and 0.36. In fact, the friction coefficient of samples covered with Ag/CaF_x multilayer films reaches an average value reflecting the friction properties of an $Ag\text{-}CaF_x$ composite material. Furthermore, SEM examinations of the wear tracks demonstrate that Ag and

CaF_x are distributed within the wear tracks and both materials act together as lubricants during tribological tests. The alumina balls are also covered with lubricant materials after tribological tests at 500°C.

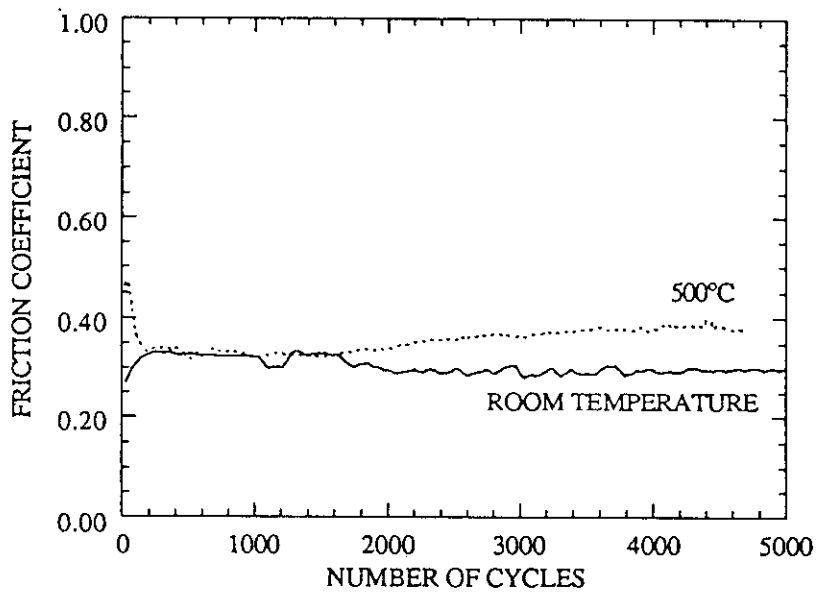

Figure 41. Friction coefficient versus number of cycles of a 47-nm-thick Ag/40-nm-thick CaF_x multilayer structure with a total thickness of 0.7 μm under a load of 1 N [87].

The Ag/CaF_x multilayer films exhibit a low friction coefficient between room temperature and 500°C. Tribological tests of these multilayer lubricant films in air at temperatures ranging from 500°C to 800°C are in progress. This type of stacked lubricant structures may offer an interesting approach for lubrication of mechanical components with high precision tolerance and reliability operating in wide temperature ranges in air.

5. Rationale for the Selection of Coating Process and Coating Material for a Given Lubrication Application

The selection and design of tribological coatings ensuring both protection against wear and low friction coefficient can be very complex. In fact, three basic aspects must be considered in the selection of a suitable tribological coating : (i) the technical function of the moving mechanical assembly, (ii) the operating conditions including load, sliding velocity, temperature and nature of ambient gas, and (iii) the type of friction, wear and lubrication mechanisms expected to occur during operation. In general, a tribological coating is a composite coating capable of ensuring various functions. Friction reduction may be the primary function of most coatings in engineering practice. Furthermore, the environment for a tribological coating in operation can impose specific requirements

regarding the interactions, function and stability of the coating. Thermal control and stress interaction problems have an impact on other functions. As mentioned by Czichos [88], mechanical stress interactions can be optimized by varying the properties of the coating from the surface to the base material; a tribological coating can be designed on the basis of the following general scheme : (i) a thin surface layer to prevent adhesion between opposing surfaces in sliding contact, e.g., this surface layer can be a solid lubricant film (ii) an intermediate layer with ductility to support Hertzian contact stress, and (iii) a subsurface material offering a transition to the properties of the bulk material [89].

Numerous interacting processes including friction, wear, environment, thermal stresses and mechanical stresses as well as a variety of operating variables that should be part of the design logic for tribological coatings have been presented and discussed in detail by Johnson [89]; from this discussion, a design logic checklist is provided at a hierarchy level that can be used by a designer and further developed by researchers.

In fact, the choice of coating materials, coating thicknesses, coating deposition techniques and other parameters must be established on a sound physical basis to ensure performance and reliability of moving mechanical assemblies in operation [90]. The primary requirement for the use of thin films in tribology is that the films exhibit a strong adherence to the substrate. In general, sputtering techniques yield films well-bounded to substrates. Besides PVD techniques, CVD techniques can also provide well-bounded films suitable for tribology; graded interfaces desirable for a strong adherence can be obtained by interdiffusion of elements in the interfacial zone during CVD processes at sufficiently high temperatures required for activation of chemical reactions involved in CVD. However, various alloys, e.g., light weight non-ferrous alloys, cannot be coated with CVD films produced at elevated temperatures since the mechanical properties and metallurgical integrity of these alloys can be degraded by thermal treatment.

The wear rate of mechanical components depends on the hardness of the counterface (rider), H_c, and hardness of the base substrate, H_s. In various cases, an increase in surface hardness of ferrous alloys by a suitable surface-hardening process is sufficient to minimize the wear rate. Improved endurance lifes of ferrous alloys in moving contact can be obtained if the hardness ratio, H_c/H_s, is in the range 0.4-0.6 [2,3]. With counterfaces made from ferrous alloys, the H_c values rarely exceed 8000 MPa; as a result, H_s values of 16000 MPa or more are desirable for negligible wear rates of the ferrous substrates. Hard compound coatings such as refractory metal nitride, carbide or boride coatings exhibit the required hardness values to serve as wear resistant coatings deposited on ferrous alloy components. However, the rider may wear rapidly with hard material coated substrates. Solid lubricant coating interposes between the sliding surfaces can lead to a reduction in wear rate of the rider.

When common engineering alloys are coated with hard material films, the effect of residual stresses must be carefully analyzed. In general, the thermal expansion coefficient, α, of hard metal compounds is lower than that of the ferrous substrates. High tensile stresses in the coatings can appear as the hard coatings are produced by CVD at elevated temperatures; hence, these stresses cause formation of cracks and other damage in the coatings. This residual stress problem is less crucial with hard coating sputter-deposited on substrates at room temperature [91].

An important factor in the choice of coating materials, namely the product of the Young's modulus by the thermal expansion coefficient, ($E\ \alpha$), appears from residual

stress considerations. Hard materials with (E α) products matching those of the substrates are required for reducing residual stress effects. With this type of hard coatings, the film-to-substrate interfacial shear stresses susceptible to appear during operation can be minimized since the differential thermal stresses are reduced. In addition, hard materials with high thermal conductivity are desirable for an efficient heat transport during sliding operation. Hence, thinner films are of particular interest to reduce thermal stresses and associated damage in sliding contact. The adjustement of (E α) products of coatings and base substrates is highly recommended for sliding contacts with high (P V) products where P is the contact pressure and V the sliding velocity. The (P V) product corresponds to the power dissipated in the sliding contact in operation. Rapid transport of the dissipated energy is necessary to reduce the surface temperature and avoid tribochemical reactions leading to corrosive wear. To avoid damage caused by tribochemical reactions, the coating material with the highest thermodynamic stability will be selected among several coating materials meeting other requirements described previously.

Finally, the more relevant physical properties to consider for the selection of coating materials include shear strength, hardness, Young's modulus, thermal expansion coefficient, thermal conductivity and thermodynamic stability in operation conditions. In addition, the thicknesses of films incorporated in the tribological composite coatings must be adjusted to optimize performance and reliability of moving mechanical systems.

The final choice among various coating materials is based on factors related to the selection of the deposition process and the ease of coating deposition. The maximum temperature needed to ensure stability of the base material restricts the allowable deposition process of coatings. Plasma-induced deposition techniques are required for high bonding strength between the coating and the substrate. Sputtering processes, activated reactive evaporation processes and plasma-induced CVD processes are the candidates which can meet the requirements [1].

6. Conclusion

The reduction in friction and wear between hard metallic components in moving mechanical assemblies operating in hostile environments where conventional fluid lubricants (oils and greases) fail can be ensured by solid lubricant coatings applied to surfaces in sliding contact. According to Amontons' law, the dynamic friction coefficient between two solids in relative moving contact is independent of the apparent area of contact, i.e., independent of the load. This law is of fairly good general validity. However, the nature of the contact between two solid surfaces is complex. The friction properties are dependent on interfacial films and surface modifications in sliding contact. Adhesion phenomena between metal surfaces play a crucial role in friction mechanisms. The role of shearing and plowing actions is considered in the Bowden-Tabor model. This friction model applied to thin solid films deposited on hard base substrates can account for much of the observed behavior.

The lubrication effect of thin solid films can be analyzed either by a macroscopic approach based on the determination of the effect of experimental parameters on the friction coefficient or by a microscopic approach of phenomena involved in the contact (interfacial rheology). Microscopic examinations of the interfaces after sliding tests are

required for a good understanding of friction mechanisms. The solid lubricant film may accomodate to sliding by three possible ways, namely intrafilm flow, interface sliding and interfacial sliding. In some cases, the situation can be more complex; a third body can form at the interface and accomodate relative motion of two solid surfaces. The general expression of the friction coefficient is composed of four terms associated with adhesion phenomena, plastic deformation of materials (plowing action), elastic deformation of materials, and third body particles, respectively. Low friction coefficients can be achieved with a variety of materials including lamellar compounds, carbon-based compounds, soft metals and inorganic compounds (metal fluorides and oxides, glasses, ...). Thin films of these lubricant materials can be deposited by PVD and CVD techniques. Strong adherence of films to base substrates is of prime importance.

In fact, a tribological coating required for reduction of friction and wear in sliding contact is a composite coating consisting of a thin surface layer to prevent adhesion between sliding surfaces, an intermediate layer with ductility to support Hertzian contact stress and a subsurface layer offering a transition to the properties of the bulk material. The selection of coating materials for a given tribological application is based on various relevant physical properties such as shear strength, hardness, Young's modulus, thermal expansion coefficient, thermal conductivity, and thermodynamic stability of materials in operation conditions. The final choice among various materials is based on factors related to the selection of the deposition process and the ease of coating deposition. For lubrication purposes, plasma-assisted deposition processes such as sputtering and plasma-enhanced CVD processes are very attractive techniques to produce adherent lubricant thin films with specific physical characteristics difficult or impossible to obtain from films produced by other deposition techniques.

7. Acknowledgements

The author is pleased to acknowledge the members of the Surface Engineering Laboratory (Nuclear Research Center of Grenoble), and Dassault Aviation Company for their helpful assistance and contribution in the course of a tribological research program on solid lubricant films operating at high temperatures funded by the European Space Agency.

8. References

1. Ramalingam, S., Shimazaki, Y., and Winer, W.O. (1981) Magnetron sputtering of non-ferrous aerospace alloys for wear protection, *Thin Solid Films* 80, 297-303.
2. Richardson, R.C.D. (1968) The wear of metals by relatively soft abrasives, *Wear* 11, 245-275.
3. Kruschov, M.M. (1974) Principles of abrasive wear, *Wear* 28, 69-88.
4. Halling, J. (1975) *Principles of Tribology*, Macmillan, London, England.
5. Bowden, F.P., and Tabor, D. (1964) *The Friction and Lubrication of Solids*, Part 2, Clarendon Press, Oxford, England.
6. Iliuc, I. (1980) *Tribology of Thin Layers*, Tribology Series, Vol.4, Elsevier Scientific Publishing Co., Amsterdam.
7. Sundgren, J.E. (1995) Hard coatings and multilayers, in Y. Pauleau (ed), *Materials and Processes for Surface and Interface Engineering*, Kluwer Academic Publishers, Dordrecht, (this volume).
8. Kragelskii, I.V., and Mikhin, N.M. (1988) *Handbook of Friction Units of Machines*, American Society of Mechanical Engineers (transl. from Russian).

9. Buckley, D.H. (1983) Importance and definition of materials in tribology : status of understanding, *Tribology in the 80's*, Vol.1, NASA Conf. Publ. 2300, National Aeronautics and Space Administration, pp.19-44.
10. Arnell, R.D., Davies, P.B., Halling, J., and Whomes, T.L. (1991) *Tribology Principles and Applications*, Springer-Verlag, Berlin, pp.1-66.
11. Rigney, D.A. (1988) Sliding wear of metals, *Ann. Rev. Mater. Sci.* 18, 141-163.
12. Binnig, G., Quate, C.F., and Gerber, C. (1986) Atomic force microscope, *Phys. Rev. Lett.* 56, 930-933.
13. Salmeron, M.B. (1993) Use of the atomic force picroscope to study mechanical properties of lubricant layers, *MRS Bull.* XVIII, 20-25.
14. Bowden, F.P., and Thomas, P.H. (1954) The surface temperature of sliding solids, *Proc. Roy. Soc. (London)* A223, 29-40.
15. Rabinowicz, E. (1971) Determination of compatibility of metals through static friction tests, *ASLE Trans.* 14, 198-205.
16. Guo, Q., Ross, J.D.J., and Pollock, H.M. (1989) What part do adhesion and deformation play in fine-scale static and sliding contact ?, in L.E. pope, L.L. Fehrenbacher, and W.O. Winer (eds), *New Materials Approaches to Tribology : Theory and Applications* 140, Materials Research Society, Pittsburgh, PA, 51-66.
17. Landman, U., Luedtke, W.D., Burnham, N., and Colton, R.J. (1990) Atomistic mechanisms and dynamics of adhesion, nanoindentation and fracture, *Science* 248, 454-461.
18. Singer, I.L. (1992) Solid lubrication processes, in I.L. Singer and H.M. Pollock (eds), *Fundamentals of Friction : Macroscopic and Microscopic Processes* E220, Kluwer Academic Publishers, Dordrecht, pp.237-261.
19. Winer, W.O., and Cheng, H.S. (1980) Film thickness, contact stress and surface temperatures, in M.B. Peterson and W.O. Winer (eds), *Wear Control Handbook*, American Society of Mechanical Engineers, pp.81-141.
20. Hardy, W., and Bircumshaw, I. (1925) Boundary Lubrication - Plane surfaces and the limitations of Amontons' law, *Proc. Roy. Soc. (London)* A108, 1-27.
21. Hardy, W. (1936) *Collected Works*, Cambridge University Press, Cambridge, England.
22. Bowden, F.P., and Tabor, D. (1950) *The Friction and Lubrication of Solids*, Part I, Clarendon Press, Oxford, England.
23. Larsen-Basse, J. (1992) Basic theory of solid friction, in P.J. Blau, S.D. Henry, G.M. Davidson, T.B. Zorc, D.R. Levicki and R.C. Uhl (eds), *Friction, Lubrication, and Wear Technology*, Handbook of the American Society of Metals, Vol.18, ASM International, pp.27-38.
24. Adamson, A.W. (1976) Friction and lubrication - adhesion, *Physical Chemistry of Surfaces*, Chap. X, John Wiley & Sons, Inc., New York, pp.426-458.
25. Burwell, J.T., and Strang, C.D. (1949) The incremental friction coefficient - A non-hydrodynamic component of boundary lubrication, *J. Appl. Phys.* 20, 79-89.
26. Fort, T. (1962) Adsorption and boundary friction on polymer surfaces, *J. Phys. Chem.* 66, 1136-1143.
27. McFarlane, J.S., and Tabor, D. (1950) Relation between friction and adhesion, *Proc. Roy. Soc. (London)* A202, 244-253.
28. Burwell, J.T., and Rabinowicz, E. (1953) The nature of the coefficient of friction, *J. Appl. Phys.* 24, 136-139.
29. Deryaguin, B.V., Karassev, V.V., Zakhavaeva, N.N., and Lazarev, V.P. (1957-58) The mechanism of boundary lubrication and the properties of the lubricating film - Short and long range action in the theory of boundary lubrication, *Wear* 1, 277-290..
30. Bowden, F.P., and Hughes, T.P. (1939) The friction of clean metals and the influence of adsorbed gases. The temperature coefficient of friction, *Proc. Roy. Soc. (London)* A172, 263-279.
31. Tingle, E.D. (1950) The importance of surface oxide films in the friction and lubrication of metals. Part I. - The dry friction of surfaces freshly exposed to air, *Trans. Faraday Soc.* 46, 93-102.
32. Bowden, F.P., and Tabor D. (1945, Pub. 1946) Friction and lubrication, *Ann. Repts. on Progress Chem. (Chem. Soc. London)* 42, 20-46.
33. Rabinowicz, E. (1965) *Friction and Wear of Materials*, John Wiley & Sons, New York.
34. Halling, J. (1979) Surface coatings - Materials conservation and optimum tribological performance, *Tribol. Int.* 12, 203-208.
35. Halling, J. (1983) The tribology of surface films, *Thin Solid Films* 108, 103-115.
36. Bowers, R.C. (1971) Coefficient of friction of high polymers as a function of pressure, *J. Appl. Phys.* 42, 4961-4970.

37. Briscoe, B.J., Scruton, B., and Willis, F.R. (1973) The shear strength of thin lubricant films, *Proc. Roy. Soc. (London)* A 333, 99-114.
38. Bowers, R.C., and Zisman, W.A. (1968) Pressure effects on the friction coefficient of thin film solid lubricants, *J. Appl. Phys.* 39, 5385-5395.
39. Roberts, E.W. (1989) Ultralow friction films of MoS_2 for space applications, *Thin Solid Films* 181, 461-473.
40. Roberts, E.W. (1990) The advantages and limitations of sputtered molybdenum disulfide as a space lubricant, Proceedings of the 4th European Symposium on Space Mechanisms and Tribology, ESA SP-299, pp.59-65.
41. Peterson, M.B., and Ramalingam, S. (1981) Coatings for tribological applications, in D.A. Rigney (ed), *Fundamentals of Friction and Wear of Materials*, American Society of Metals, Metals Park , OH, pp.331-372.
42. Peterson, M.B., Murray, S.F., and Florek, J.J. (1960) Consideration of lubricants for temperatures above 1000 F, *ASLE Trans.* 2, 225-234.
43. Ives, L.K., and Peterson, M.B. (1985) in F.F. Ling (ed), *Fundamentals of High-Temperature Friction and Wear with Emphasis on Solid Lubrication for Heat Engines*, Indust. Tribology Inst., Troy, NY, pp.43.
44. Berthier, Y., Vincent, L., and Godet, M. (1988) Velocity accomodation in fretting, *Wear* 125, 25-38.
45. Berthier, Y., Godet, M., and Brendle, M. (1989) Velocity accomodation in friction, *Tribol. Trans.* 32, 490-496.
46. Singer, I.L. (1991) A thermochemical model for analyzing low wear-rate materials, *Surf. Coat. Technol.* 49, 474-481.
47. Cooper, H.S., and Damerell, V.R. (1939) Lubricants suitable for various uses, U.S. Patent 2,156,803.
48. Bell, M.E. and Findlay, J.H. (1941) Molybdenite as a new lubricant, *Phys. Rev.* 59, 922.
49. Winer, W.O. (1967) Molybdenum disulfide as a lubricant : a review of the fundamental knowledge, *Wear* 10, 422-452.
50. Sliney, H.E. (1982) Solid lubricant materials for high temperatures - a review, *Tribol. Int.* 15, 303-315.
51. Sliney, H.E. (1992) Solid lubricants, in P.J. Blau, S.D. Henry, G.M. Davidson, T.B. Zorc, D.R. Levicki and R.C. Uhl (eds), *Friction, Lubrication, and Wear Technology*, ASM Handbook, Vol.18, ASM International, pp.113-122.
52. Lancaster, J.K. (1984) Solid lubricants, in E.R. Booser (ed), *Handbook of Lubrication : Theory and Design*, Vol II, CRC Press, Boca Raton, FL, pp.267-290.
53. Sutor, P. (1991) Solid lubricants : overview and recent developments, *MRS Bull.* XVI, 24-30.
54. Singer, I.L. (1989) Solid lubricating films for extreme environments, in L.E. Pope, L.L. Fehrenbacher and W.O. Winer, *New Approaches to Tribology : Theory and Applications*, Vol. 140, Materials Research Society, Pittsburgh, PA, pp.215-226.
55. Sliney, H.E. (1966) Self-lubricating composites of porous nickel and nickel-chromium alloy impregnated with barium fluoride-calcium fluoride eutectic, *ASLE Trans.* 9, 336-347.
56. O'Keefe, M.J., and Rigsbee, J.M. (1995) The science, technology and materials applications of physical vapor deposition processes, in Y. Pauleau (ed), *Materials and Processes for Surface and Interface Engineering*, Kluwer Academic Publishers, Dordrecht, (this volume).
57. Wahl, G. (1995) Conventional and novel chemical vapor deposition techniques - coating methods to protect materials against hostile environments, in Y. Pauleau (ed), *Materials and Processes for Surface and Interface Engineering*, Kluwer Academic Publishers, Dordrecht, (this volume).
58. Bergmann, E., Melet, G., Müller, C., and Simon-Vermot, A. (1981) Friction properties of sputtered dichalcogenide layers, *Tribol. Int.* 14, 329-332.
59. Spalvins, T. (1987) A review of recent advances in solid film lubrication, *J. Vac. Sci. Technol. A* 5, 212-219.
60. Spalvins, T. (1982) Morphological and frictional behavior of sputtered MoS_2 films, *Thin Solid Films* 96, 17-24.
61. Stupp, B.C. (1981) Synergetic effects of metals co-sputtered with MoS_2, *Thin Solid Films* 84, 257-266.
62. Spalvins, T. (1984) Frictional and morphological properties of Au-MoS_2 films sputtered from a compact target, *Thin Solid Films* 118, 375-384.
63. Stupp, B.C. (1984) Performance of conventionally sputtered MoS_2 versus co-sputtered MoS_2 and nickel, 3rd International Conference on Solid Lubrication, ASLE SP-14, pp.217-222.
64. Spalvins, T. (1980) Tribological properties of sputtered MoS_2 films in relation to film morphology, *Thin Solid Films* 73, 291-297.

65. Niederhäuser, P., Hintermann, H.E., and Maillat, M. (1983) Moisture-resistant MoS_2-based composite lubricant films, *Thin Solid Films* **108**, 209-218.
66. Hirano, M., and Miyake, S. (1985) Sliding life enhancement of a WS_2 sputtered film by ion beam mixing, *Appl. Phys. Lett.* **47**, 683-685.
67. Chevallier, J., Olesen, S., Sorensen, G., and Gupta, B. (1986) Enhancement of sliding life of MoS_2 films deposited by combining sputtering and high-energy ion implantation, *Appl. Phys. Lett.* **48**, 876-877.
68. Hilton, M.R., and Fleischauer, P.D. (1992) Lubricants for high-vacuum applications, in P.J. Blau, S.D. Henry, G.M. Davidson, T.B. Zorc, D.R. Levicki and R.C. Uhl (eds), *Friction, Lubrication, and Wear Technology*, ASM Handbook, Vol.18, ASM International, pp.150-161.
69. Fusaro, R.L., and Sliney, H.E. (1970) Graphite fluoride $(CF_x)_n$ - a new solid lubricant, *ASLE Trans.* **13**, 56-65.
70. Harrop, R., and Harrop, P.J. (1969) Friction of sputtered PTFE films, *Thin Solid Films* **3**, 109-117.
71. Dimigen, H., and Hübsch, H. (1983/84) Applying low-friction wear-resistant thin solid films by physical vapour deposition, *Philips Techn. Rev.* **41**, 186-197.
72. Miyake, S. (1992) Tribological properties of hard carbon films : extremely low friction mechanism of amorphous hydrogenated carbon films and amorphous hydrogenated SiC films in vacuum, *Surf. Coat. Technol.* **54/55**, 563-569.
73. Miyake, S., and Takahashi, S. (1987) Small-angle oscillatory performance of solid-lubricant film-coated ball bearings for vacuum applications, *ASLE Trans.* **30**, 248-253.
74. Miyake, S., Takahashi, S., Watanabe, I., and Yoshihara, H. (1987) Friction and wear behavior of hard carbon films, *ASLE Trans.* **30**, 121-127.
75. Sugimoto, I., and Miyake, S. (1990) Oriented hydrocarbons transferred from a high performance lubricative amorphous C:H:Si film during sliding in a vacuum, *Appl. Phys. Lett.* **56**, 1868-1870.
76. Matsuo, S., and Kiuchi, M. (1982) Low temperature deposition apparatus using electron cyclotron resonance plasma, in C.J. Dell'Oca and W.M. Bullis (eds), *Proceedings of the 1st International Symposium on Very Large Scale Integration Science and Technology*, Vol.82-7, The Electrochemical Society Inc., Pennington, NJ, pp.79-86.
77. Spalvins, T., and Buzek, B. (1981) Frictional and morphological characteristics of ion-plated soft metallic films, *Thin Solid Films* **84**, 267-272.
78. D'Heurle, F.M., and Harper, J.M.E. (1989) Note on the origin of intrinsic stresses in films deposited via evaporation and sputtering, *Thin Solid Films* **171**, 81-92.
79. Maréchal, N., Quesnel, E., and Pauleau, Y. (1994) Silver thin films deposited by magnetron sputtering, *Thin Solid Films* **241**, 34-38.
80. Maréchal, N., Quesnel, E., and Pauleau, Y. (1994) Characterization of silver films deposited by radio frequency magnetron sputtering, *J. Vac. Sci. Technol. A* **12**, 707-713.
81. Maréchal, N., Quesnel, E., and Pauleau, Y. (1994) Properties of silver films sputter-deposited on biased substrates, *J. Electrochem. Soc.* **141**, 1691-1698.
82. Maréchal, N., Quesnel, E., Juliet, P., Pauleau, Y., and Zimmermann, C. (1994) Tribological properties of silver thin films sputter-deposited on superalloy substrates, Thin Solid Films 249, 70-77.
83. Smithells, C.J. (1976) *Metal Reference Book*, 5th Edition, Butterworth, London, England.
84. Phillips, W.L., Jr. (1961) Deformation and fracture processes in calcium fluoride single crystals, *J. Am. Ceram. Soc.* **44**, 499-506.
85. Burn, R., and Murray, G.T. (1962) Plasticity and dislocation etch pits in CaF_2, *J. Am. Ceram. Soc.* **45**, 251-252.
86. Maréchal, N., Quesnel, E., Juliet, P., and Pauleau, Y. (1993) Radio frequency sputter-deposition and properties of calcium fluoride thin films, *J. Appl. Phys.* **74**, 5203-5211.
87. Maréchal, N., Pauleau, Y., Quesnel, E., Juliet, P., Rouzaud, A., and Zimmermann, C. (1994) Sputter-deposited lubricant thin films operating at elevated temperatures in air, *Surf. Coat. Technol.* **68/69**, 416-421.
88. Czichos, H. (1978) *A Systems Approach to the Science and Technology of Friction, Lubrication and Wear*, Elsevier, New York.
89. Johnson, R.L. (1980) A systems rationale for the selection or design of tribological surface coatings, *Thin Solid Films* **73**, 235-244.
90. Ramalingam, S. (1984) Tribological characteristics of thin films and applications of thin film technology fro friction and wear reduction, *Thin Solid Films* **118**, 335-349.
91. Nakamura, K., Inagawa, K., Tsuruoka, K., and Komiya, S. (1977) Applications of wear-resistant thick films formed by physical vapor deposition processes, *Thin Solid Films* **40**, 155-167.